Electronic Supplementary Material (ESI) for Inorganic Chemistry Frontiers.


**Electronic Supplementary Information (ESI)**

# Synthesis of carboxy-cyclobutane Isomers combining amide bond and self-assembly of coordination polymers in solid state : Controlling the reaction site of [ 2+ 2] cycloaddition by introducing a substituent group

Rong-Rong Zhu, [a] Tao Wang, [a] LiJia Zhao, [a] Liancheng He, [a] Feng Gao, [a,b] Lin Du*[a,b] and Qi-Hua Zhao*[a,b]

[a]School of Chemical Science and Technology, Yunnan University, Kunming 650091, People's Republic of China.

[b]Key Laboratory of Medicinal Chemistry for Natural Resource, Ministry of Education, Yunnan Research & Development Center for Natural Products, Yunnan University, Kunming 650091, People's Republic of China.

* Corresponding author.

E-mail: qhzhao@ynu.edu.cn; lindu@ynu.edu.cn

**Table of Contents**

## Experimental

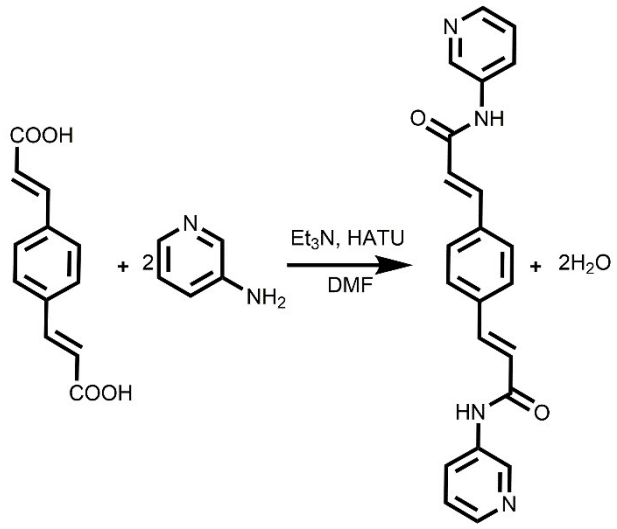


**Scheme S1** Synthesis of pbpa.

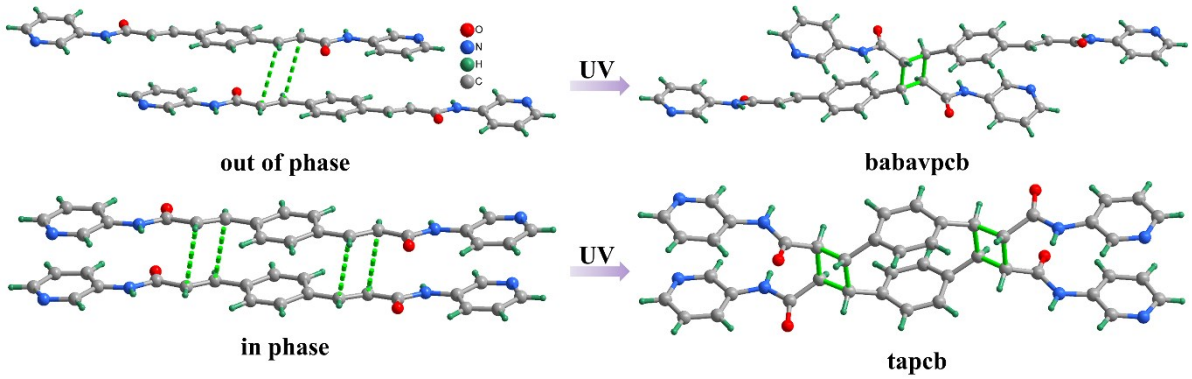


**Scheme S2** Two different alignments of pbpa ligands, which result in the formation of responsing photoproducts under UV irradiation.

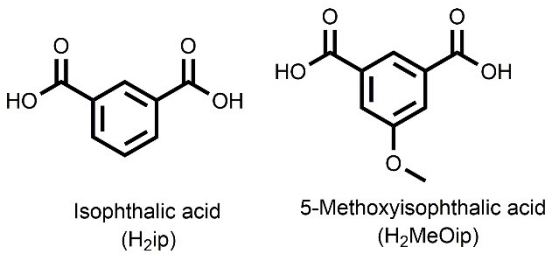


**Scheme S3** Strustures of isophthalic acid and 5-Methoxyisophthalic acid, the carboxylic acids used in this work.

**Table S1** Crystallographic data and structure refinement summary for **pbpa** and **1**-**2a**.

| Compound | pbpa | 1 | 1a | 2 | 2a |
|---|---|---|---|---|---|
| CCDC number | 2031703 | 2031704 | 2031705 | 2031706 | 2031707 |
| Empirical formula | $C_{22}H_{22}N_4O_4$ | $C_{60}H_{54}Cd_2N_8O_{17}$ | $C_{60}H_{54}Cd_2N_8O_{17}$ | $C_{31}H_{30}CdN_4O_{10}$ | $C_{31}H_{30}CdN_4O_{10}$ |
| Formula weight | 406.43 | 1383.91 | 1383.91 | 730.99 | 730.99 |
| Temperature/K | 110(2) | 293.15 | 293(2) | 100(2) | 150.0 |
| Crystal system | Monoclinic | Triclinic | Triclinic | Triclinic | Triclinic |
| Space group | $P2_1/n$ | $P\bar{1}$ | $P\bar{1}$ | $P\bar{1}$ | $P\bar{1}$ |
| a/Å | 4.6257(3) | 10.1695(13) | 10.310(3) | 10.3164(3) | 10.4338(3) |
| b/Å | 22.0943(15) | 10.4856(14) | 11.101(3) | 11.5498(3) | 11.3666(3) |
| c/Å | 10.1647(6) | 14.2567(18) | 13.809(3) | 13.9452(4) | 13.9471(4) |
| α/° | 90 | 87.806(2) | 106.513(3) | 113.1120(10) | 113.5200(10) |
| β/° | 102.715(2) | 73.590(2) | 90.714(3) | 92.1050(10) | 92.3600(10) |
| γ/° | 90 | 85.321(2) | 95.475(3) | 96.5960(1) | 94.6500(10) |
| Volume/Å³ | 1013.37(11) | 1453.3(3) | 1507.1(7) | 1512.03(7) | 1506.77(7) |
| Z | 2 | 1 | 1 | 2 | 2 |
| $\rho_{calc}$g/cm$^3$ | 1.332 | 1.581 | 1.525 | 1.606 | 1.611 |
| μ/mm$^{-1}$ | 0.094 | 0.811 | 0.783 | 0.788 | 0.791 |
| F(000) | 428.0 | 702.0 | 702.0 | 744.0 | 744.0 |
| Crystal size/mm³ | 0.19×0.15×0.12 | 0.20×0.16×0.12 | 0.26×0.20×0.16 | 0.17×0.14 ×0.11 | 0.15×0.12 ×0.09 |
| Crystal shape | Needle | Block | Block | Block | Block |
| Radiation | MoKα (λ = 0.71073) | MoKα (λ = 0.71073) | MoKα (λ = 0.71073) | MoKα (λ = 0.71073) | MoKα (λ = 0.71073) |
| 2Θ range for data collection/° | 4.502–55.032 | 4.868–56.844 | 3.078–56.278 | 5.156–55.096 | 4.862–52.828 |
| Index ranges | -5 ≤ h ≤ 6, -28 ≤ k ≤ 28, -12 ≤ l ≤ 13 | -13 ≤ h ≤ 13, -13 ≤ k ≤ 13, -19 ≤ l ≤ 18 | -13 ≤ h ≤ 13, -14 ≤ k ≤ 14, -18 ≤ l ≤ 18 | -13 ≤ h ≤ 13, -14 ≤ k ≤ 15, -18 ≤ l ≤ 18 | -12 ≤ h ≤ 13, -13 ≤ k ≤ 14, -17 ≤ l ≤ 17 |
| Reflections collected | 8162 | 13886 | 14241 | 18512 | 17422 |
| Independent reflections | 2245 [$R_{int}$ = 0.0516, $R_{sigma}$ = 0.0529] | 6667 [$R_{int}$ = 0.0463, $R_{sigma}$ = 0.0828] | 6817 [$R_{int}$ = 0.0658, $R_{sigma}$ = 0.1198] | 6881 [$R_{int}$ = 0.0390, $R_{sigma}$ = 0.0479] | 6147 [$R_{int}$ = 0.0477, $R_{sigma}$ = 0.0595] |
| Data/restrains/parameters | 2245/0/197 | 6667/1/403 | 6817/0/509 | 6881/0/569 | 6147/18/433 |
| Goodness-of-fit on $F^2$ | 1.071 | 0.976 | 0.968 | 1.075 | 1.136 |
| Final R indexes [I>=2σ(I)] | $R_1$ = 0.0474, $wR_2$ = 0.0914 | $R_1$ = 0.0464, $wR_2$ = 0.0888 | $R_1$ = 0.0584, $wR_2$ = 0.1267 | $R_1$ = 0.0400, $wR_2$ = 0.0916 | $R_1$ = 0.0514, $wR_2$ = 0.1232 |
| Final R indexes [all data] | $R_1$ = 0.0814, $wR_2$ = 0.1086 | $R_1$ = 0.0772, $wR_2$ = 0.1024 | $R_1$ = 0.1327, $wR_2$ = 0.1679 | $R_1$ = 0.0441, $wR_2$ = 0.0941 | $R_1$ = 0.0724, $wR_2$ = 0.1368 |
| Largest diff. peak/hole / e·Å³ | 0.18/-0.23 | 0.98/-0.89 | 0.72/-1.07 | 1.06/-0.93 | 1.80/-0.86 |

**Table S2** Selected Bond Distances (Å) and Angles (deg) for **1**-**2a.**

| **1** | | | |
|---|---|---|---|
| Cd1—O3$^{i}$ | 2.225 (3) | O3$^{i}$—Cd1—O1 | 96.33 (10) |
| Cd1—N4$^{ii}$ | 2.280 (3) | N4$^{ii}$—Cd1—O1 | 101.12 (10) |
| Cd1—N1 | 2.295 (3) | N1—Cd1—O1 | 94.41 (10) |
| Cd1—O1 | 2.340 (3) | O3$^{i}$—Cd1—O2 | 151.19 (10) |
| Cd1—O2 | 2.427 (2) | N4$^{ii}$—Cd1—O2 | 90.60 (9) |
| Cd1—O3W | 2.496 (6) | N1—Cd1—O2 | 89.93 (10) |
| Cd1···O3W | 2.566 (6) | O1—Cd1—O2 | 54.87 (9) |
| O3—Cd1$^{iii}$ | 2.225 (3) | O3$^{i}$—Cd1—O3W | 126.50 (13) |
| N4—Cd1$^{iv}$ | 2.280 (3) | N4$^{ii}$—Cd1—O3W | 80.79 (17) |
| O3$^{i}$—Cd1—N4$^{ii}$ | 95.25 (10) | N1—Cd1—O3W | 80.81 (17) |
| O3$^{i}$—Cd1—N1 | 93.24 (10) | O1—Cd1—O3W | 136.99 (12) |
| N4$^{ii}$—Cd1—N1 | 161.34 (11) | O2—Cd1—O3W | 82.27 (13) |
| **1a** | | | |
| Cd1—O3$^{i}$ | 2.239 (4) | O3$^{i}$—Cd1—O1 | 89.38 (14) |
| Cd1—N1 | 2.294 (4) | N1—Cd1—O1 | 93.41 (14) |
| Cd1—N4$^{ii}$ | 2.300 (4) | N4$^{ii}$—Cd1—O1 | 101.74 (15) |
| Cd1—O1 | 2.341 (4) | O3$^{i}$—Cd1—O2 | 144.32 (16) |
| Cd1—O2 | 2.416 (3) | N1—Cd1—O2 | 89.06 (14) |
| Cd1—O3W | 2.454 (8) | N4$^{ii}$—Cd1—O2 | 89.66 (14) |
| Cd1···O3W | 2.746 (1) | O1—Cd1—O2 | 54.99 (13) |
| O3—Cd1$^{iii}$ | 2.239 (4) | O3$^{i}$—Cd1—O3W | 110.1 (2) |
| N4—Cd1$^{iv}$ | 2.300 (4) | N1—Cd1—O3W | 82.7 (3) |
| O3$^{i}$—Cd1—N1 | 95.65 (14) | N4$^{ii}$—Cd1—O3W | 78.9 (3) |
| O3$^{i}$—Cd1—N4$^{ii}$ | 96.70 (15) | O1—Cd1—O3W | 160.39 (19) |
| N1—Cd1—N4$^{ii}$ | 160.49 (16) | O2—Cd1—O3W | 105.6 (2) |
| **2** | | | |
| Cd1—N1 | 2.274 (3) | N1—Cd1—O2$^{ii}$ | 90.58 (9) |
| Cd1—N4$^{i}$ | 2.278 (3) | N4$^{i}$—Cd1—O2$^{ii}$ | 87.59 (9) |
| Cd1—O1 | 2.309 (2) | O1—Cd1—O2$^{ii}$ | 134.48 (8) |
| Cd1—O2$^{ii}$ | 2.326 (2) | N1—Cd1—O3$^{iii}$ | 95.19 (9) |
| Cd1—O3$^{iii}$ | 2.415 (2) | N4$^{i}$—Cd1—O3$^{iii}$ | 91.29 (9) |
| Cd1—O4$^{iii}$ | 2.419 (2) | O1—Cd1—O3$^{iii}$ | 138.97 (8) |
| O2—Cd1$^{ii}$ | 2.326 (2) | O2$^{ii}$—Cd1—O3$^{iii}$ | 86.51 (8) |
| O4—Cd1$^{iv}$ | 2.419 (2) | N1—Cd1—O4$^{iii}$ | 93.64 (9) |
| O3—Cd1$^{iv}$ | 2.415 (2) | N4$^{i}$—Cd1—O4$^{iii}$ | 91.98 (9) |
| N1—Cd1—N4$^{i}$ | 173.14 (9) | O1—Cd1—O4$^{iii}$ | 85.07 (8) |
| N1—Cd1—O1 | 87.28 (9) | O2$^{ii}$—Cd1—O4$^{iii}$ | 140.41 (8) |
| N4$^{i}$—Cd1—O1 | 89.29 (9) | O3$^{iii}$—Cd1—O4$^{iii}$ | 53.90 (7) |
| **2a** | | | |

| | | | |
|---|---|---|---|
| Cd1—O1 | 2.272 (3) | O1—Cd1—C30$^{ii}$ | 118.01 (13) |
| Cd1—O2$^{i}$ | 2.325 (3) | O2$^{i}$—Cd1—O4$^{ii}$ | 84.93 (12) |
| Cd1—O4$^{ii}$ | 2.398 (3) | O2$^{i}$—Cd1—O3$^{ii}$ | 138.86 (11) |
| Cd1—O3$^{ii}$ | 2.414 (4) | O2$^{i}$—Cd1—C30$^{ii}$ | 111.84 (13) |
| Cd1—N4$^{iii}$ | 2.288 (4) | O4$^{ii}$—Cd1—O3$^{ii}$ | 54.15 (11) |
| Cd1—N1 | 2.288 (4) | O4$^{ii}$—Cd1—C30$^{ii}$ | 26.98 (12) |
| O2—Cd1$^{i}$ | 2.325 (3) | O3$^{ii}$—Cd1—C30$^{ii}$ | 27.18 (12) |
| O4—Cd1$^{iv}$ | 2.398 (3) | N4$^{iii}$—Cd1—O2$^{i}$ | 85.39 (13) |
| O3—Cd1$^{iv}$ | 2.414 (4) | N4$^{iii}$—Cd1—O4$^{ii}$ | 90.37 (12) |
| N4—Cd1$^{v}$ | 2.288 (4) | N4$^{iii}$—Cd1—O3$^{ii}$ | 90.28 (13) |
| O1—Cd1—O2$^{i}$ | 130.08 (12) | N4$^{iii}$—Cd1—N1 | 173.76 (14) |
| O1—Cd1—O4$^{ii}$ | 144.98 (12) | N1—Cd1—O2$^{i}$ | 89.54 (13) |
| O1—Cd1—O3$^{ii}$ | 90.86 (12) | N1—Cd1—O4$^{ii}$ | 92.80 (13) |
| O1—Cd1—N4$^{iii}$ | 91.44 (12) | N1—Cd1—O3$^{ii}$ | 95.93 (14) |
| O1—Cd1—N1 | 89.04 (13) | | |

Symmetry codes, for 1: (i) *x*, *y*-1, *z*; (ii) *x*-1, *y*-1, *z*-1; (iii) *x*, *y*+1, *z*; (iv) *x*+1, *y*+1, *z*+1; for 1a: (i) x-1, y, z; (ii) x+1, y-1, z+1; (iii) x+1, y, z; (iv) x-1, y+1, z-1; (v) -x-1, -y+3, -z; for 2: (i) x+1, y+2, z+1; (ii) -x+1, -y+2, -z+2; (iii) x-1, y, z; (iv) x+1, y, z; (v) x-1, y-2, z-1; for 2a: (i) -x+1, -y, -z; (ii) x+1, y, z; (iii) x-1, y-2, z-1; (iv) x-1, y, z; (v) x+1, y+2, z+1; (vi) -x+2, -y+2, -z+1; (vii) -x+1, -y+1, -z.

## Results and Discussion

### Crystal structures

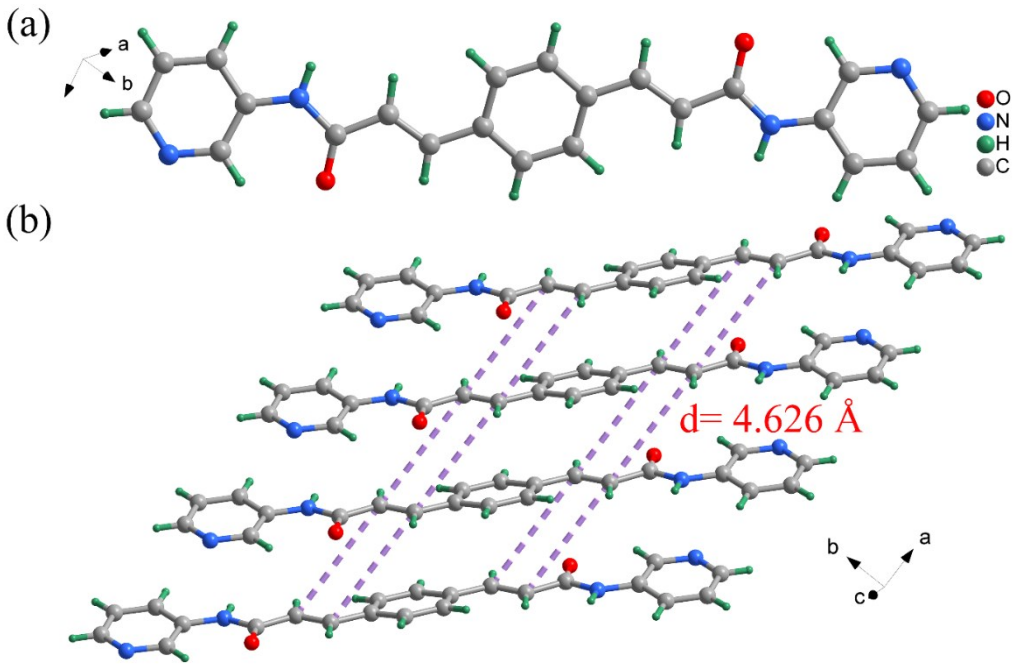


**Fig. S1** (a) Crystal structure of pbpa. (b) Distance between adjacent olefins in pbpa crystals. The non-coordinated solvent molecules are omitted.

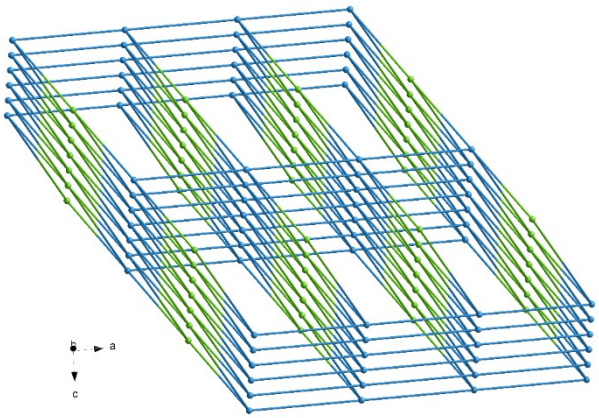

**Fig. S2** Binoda **fsc** topology with point symbol of $\{4^4\cdot6^{10}\cdot8\}\{4^4\cdot6^2\}$ in **1a**.

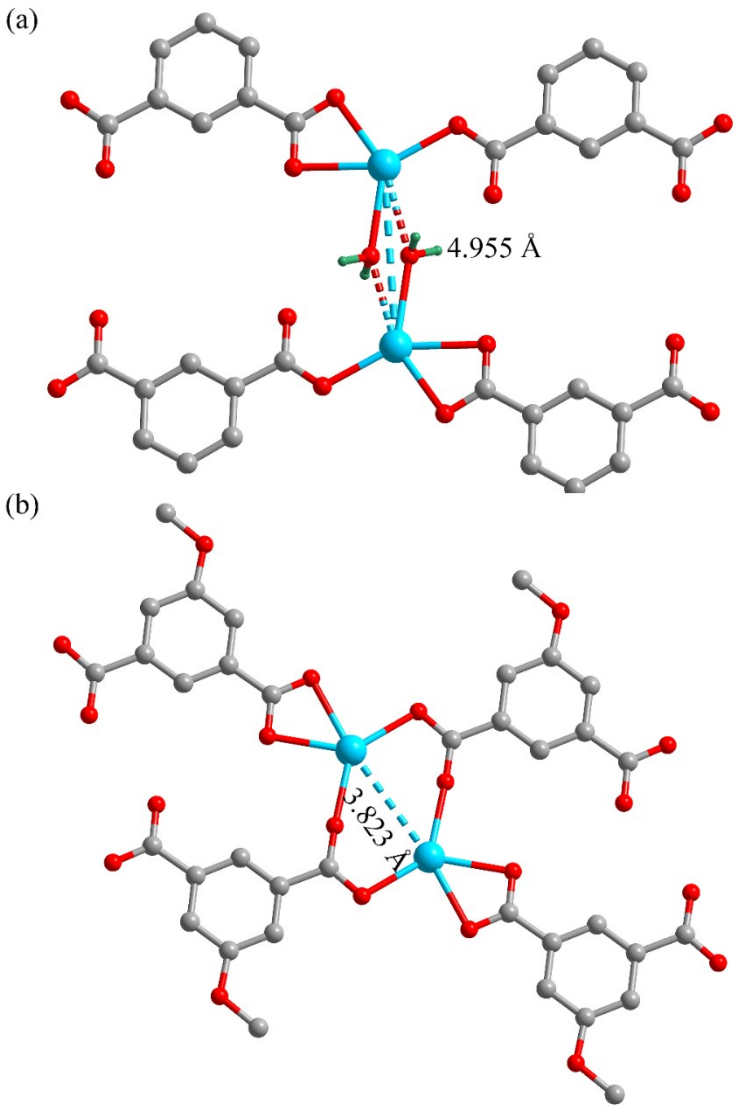


**Fig. S3** Cd···Cd distance and component of the 1D carboxyl chain in **1** (a) and **2** (b).

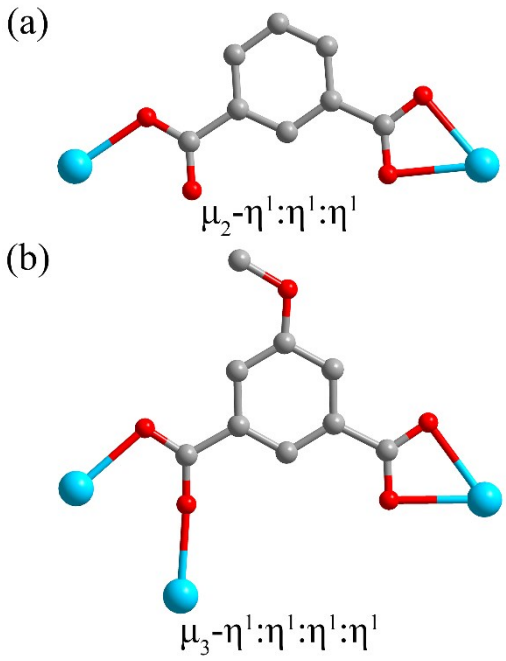


**Fig. S4** Coordination modes of the carboxyl ligands in **1** (a) and **2** (b).

**PXRD**

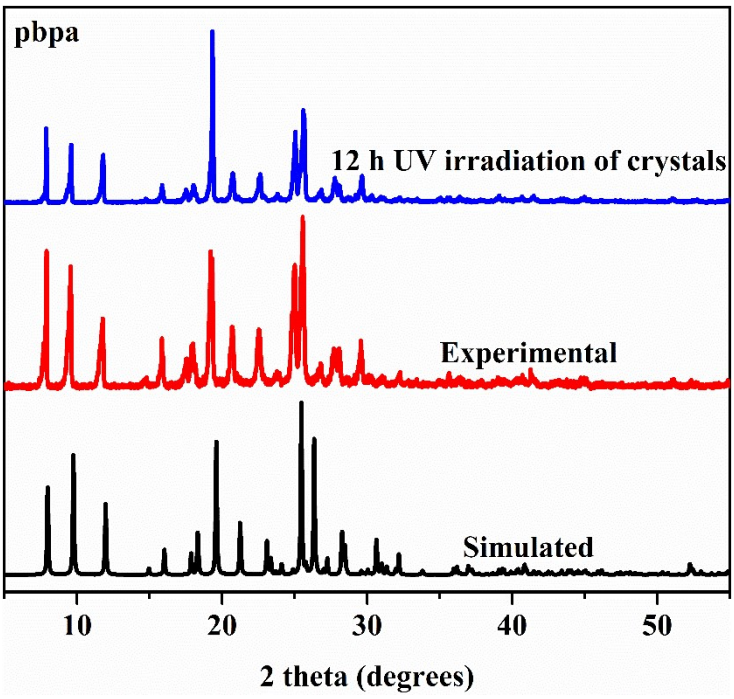


**Fig. S5** PXRD patterns of pbpa.

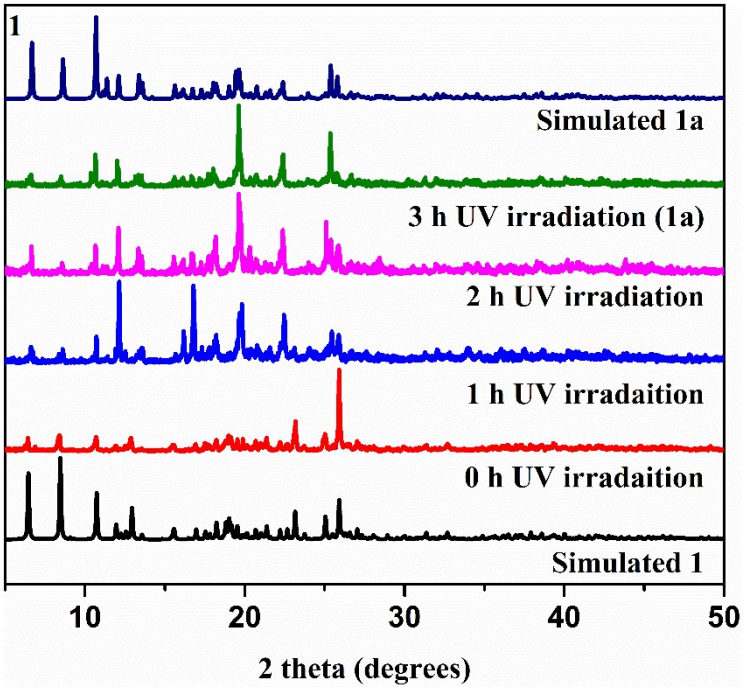


**Fig. S6** PXRD patterns of **1**–**1a**.

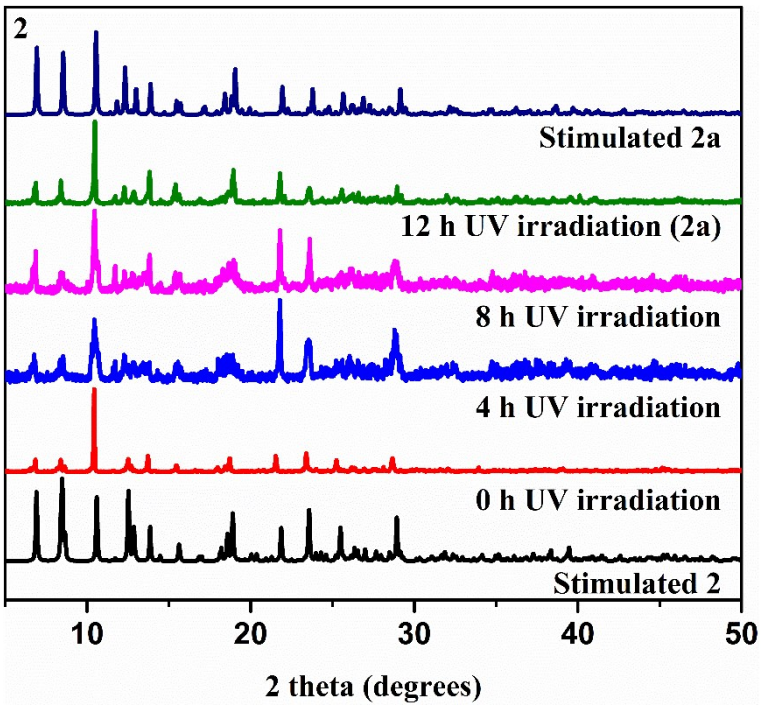


**Fig. S7** PXRD patterns of **2**–**2a**.

**NMR spectra**

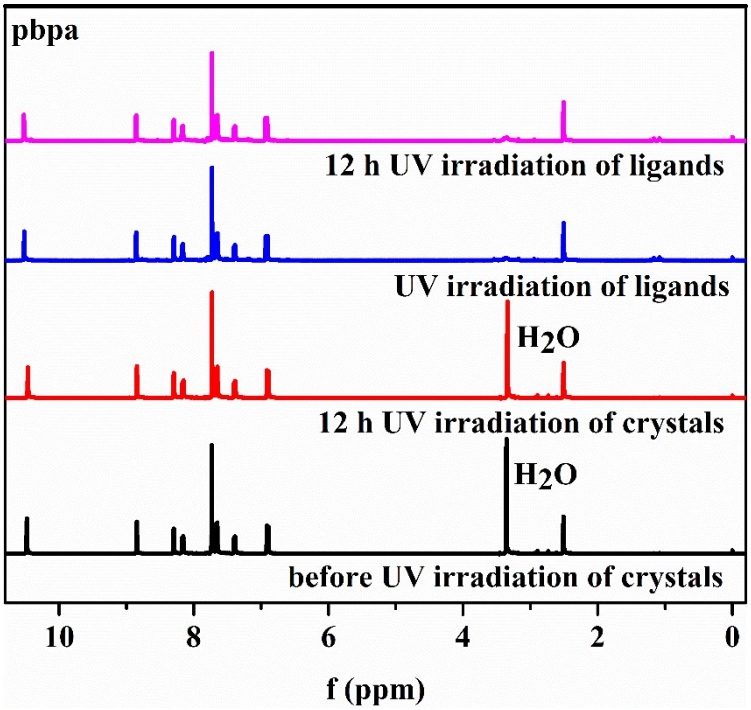


**Fig. S8** $^1$H-NMR patterns of **pbpa** ligands and crystals in DMSO-$d_6$subjected to UV irradiation at 0 and 12 h.

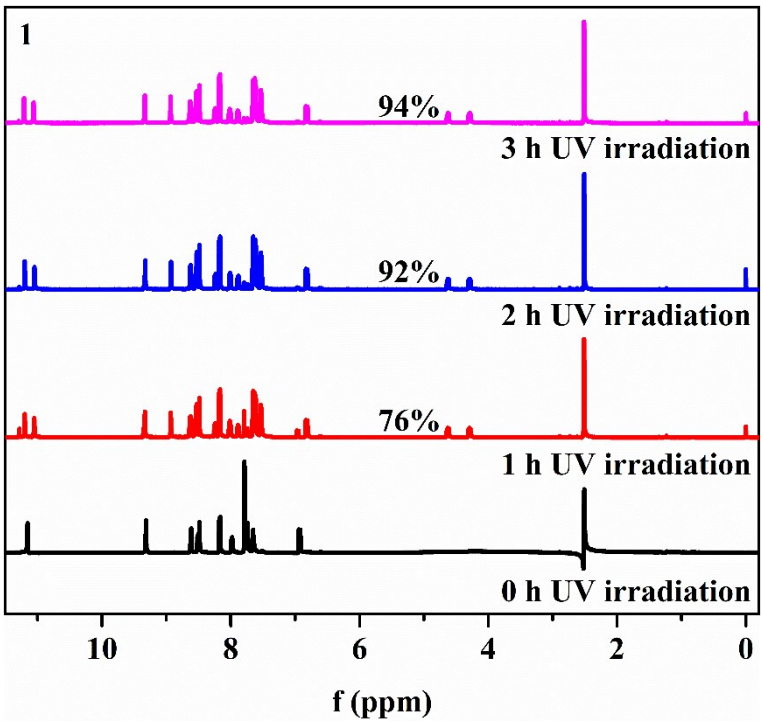


**Fig. S9** $^1$H-NMR patterns of **1** in DMSO-$d_6$subjected to UV irradiation at same interval of time.

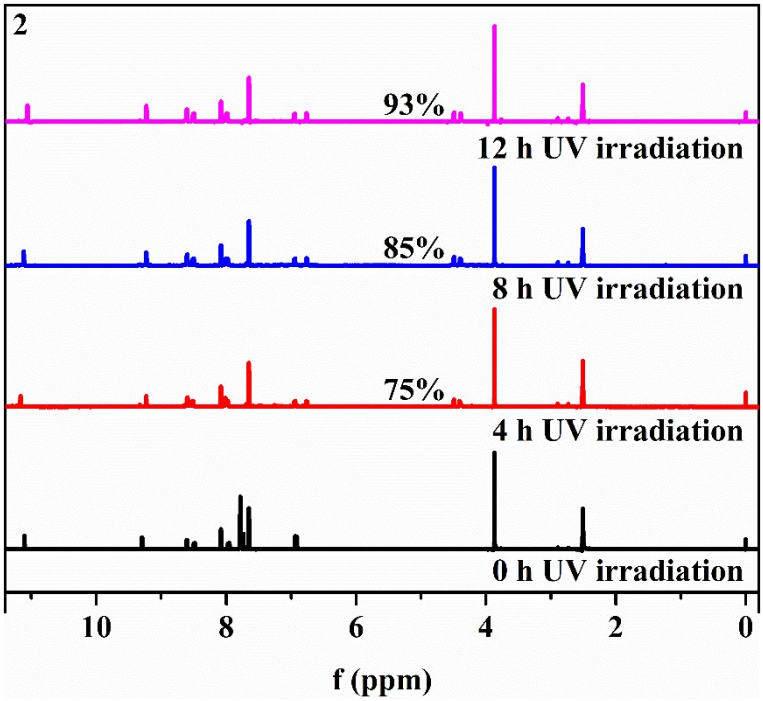


**Fig. S10** $^{1}$H-NMR patterns of **2** in DMSO-$d_6$subjected to UV irradiation at same interval of time.

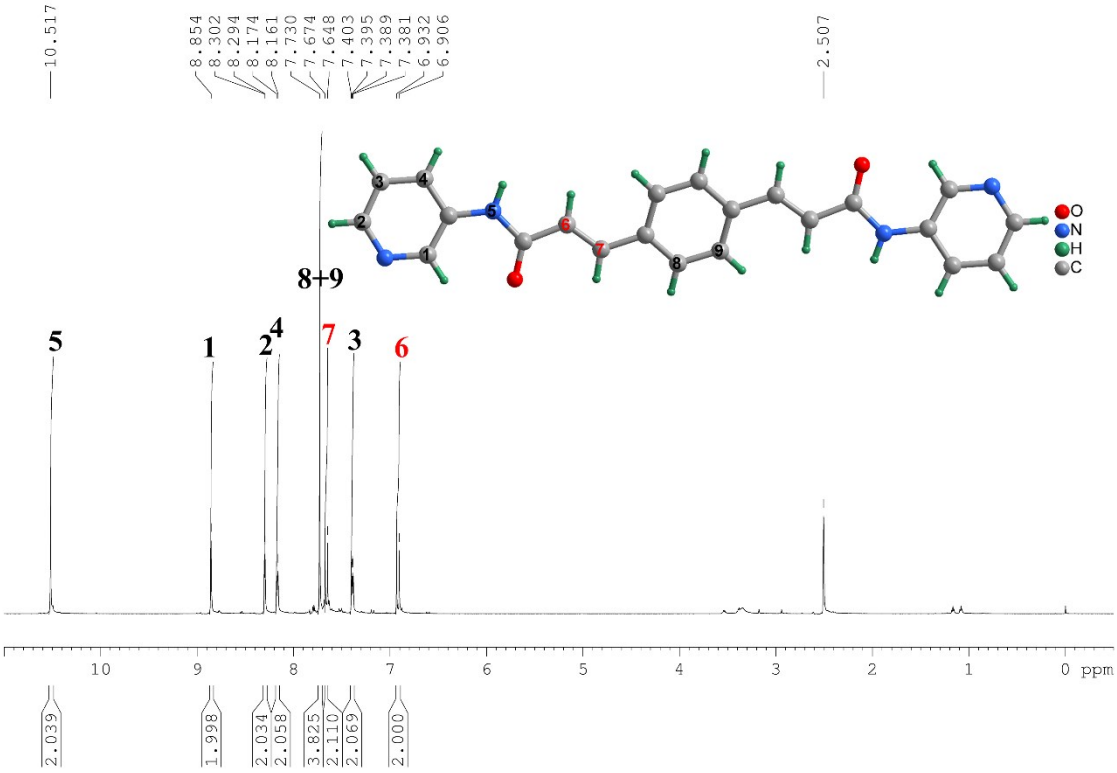


**Fig. S11** $^{1}$H-NMR spectrum of **pbpa** in DMSO-$d_6$.

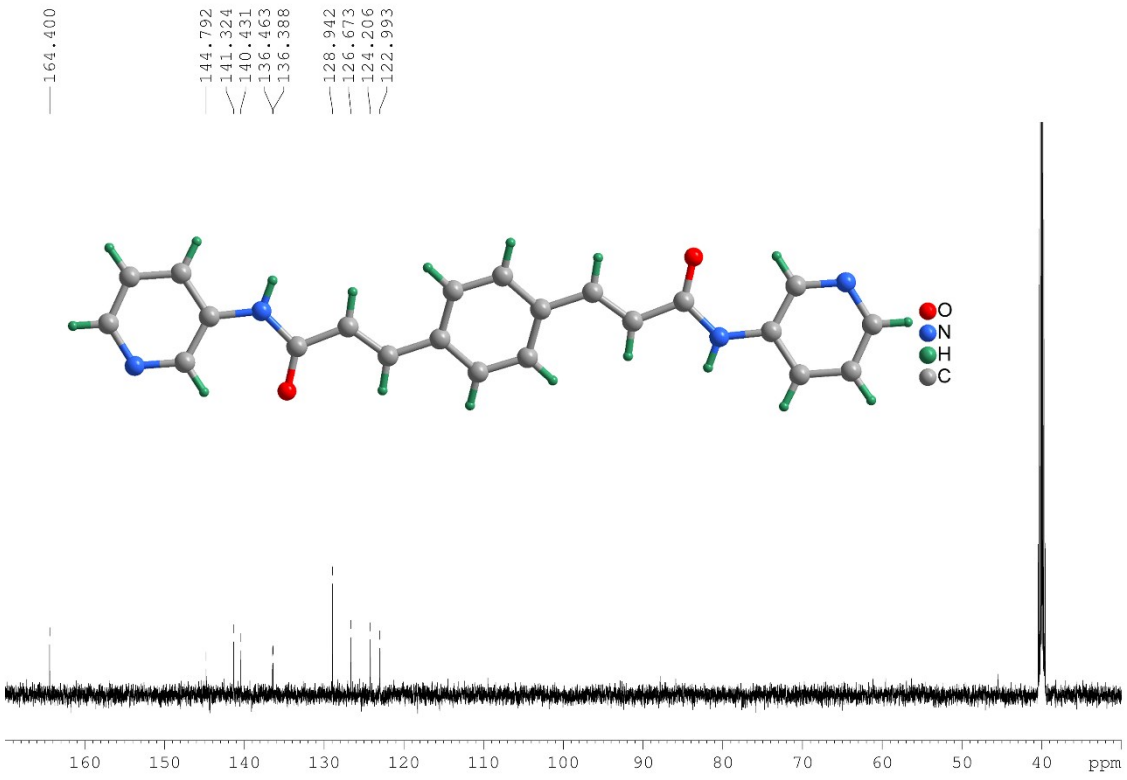


**Fig. S12** $^{13}$C-NMR spectrum of **pbpa** in DMSO-$d_6$.

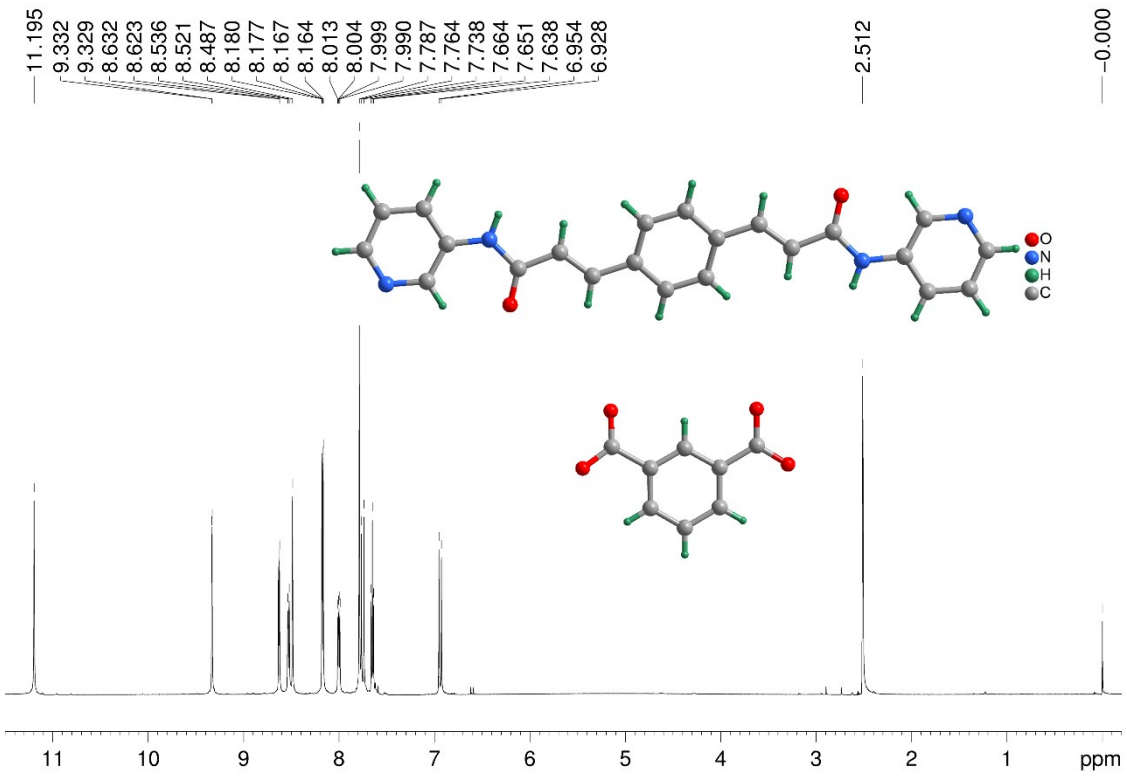


**Fig. S13** $^{1}$H-NMR spectrum of **1** in DMSO-$d_6$.

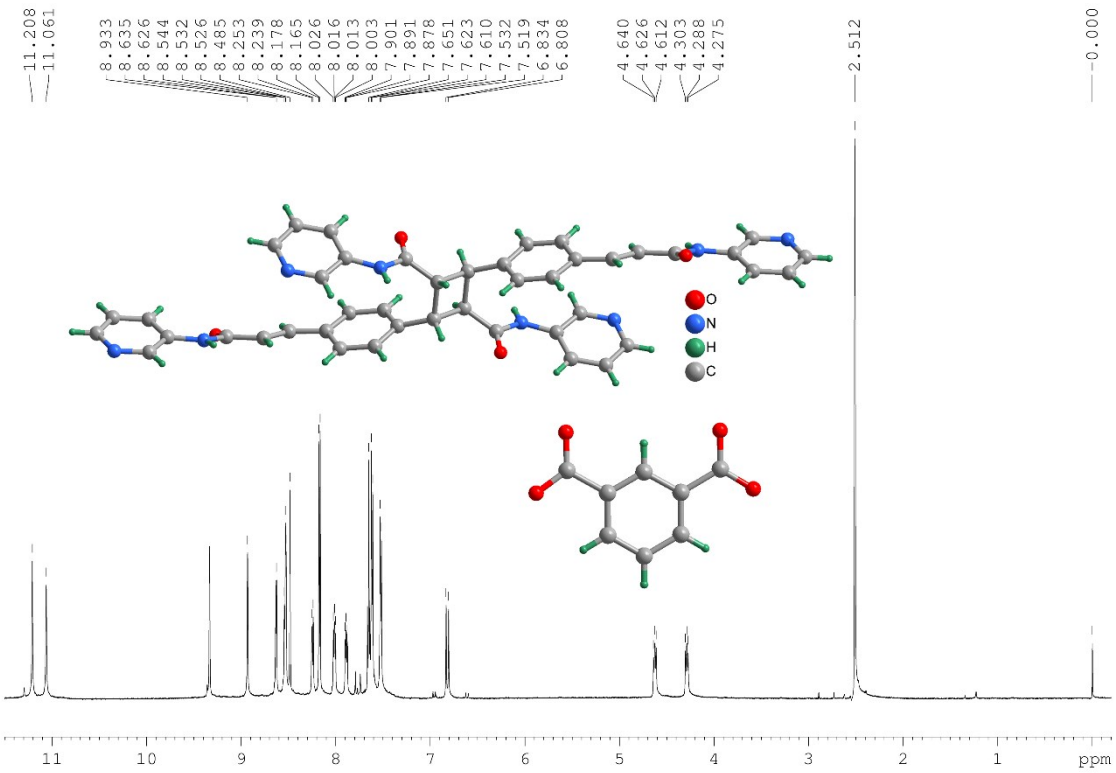


**Fig. S14** $^{1}$H-NMR spectrum of **1a** in DMSO-$d_6$.

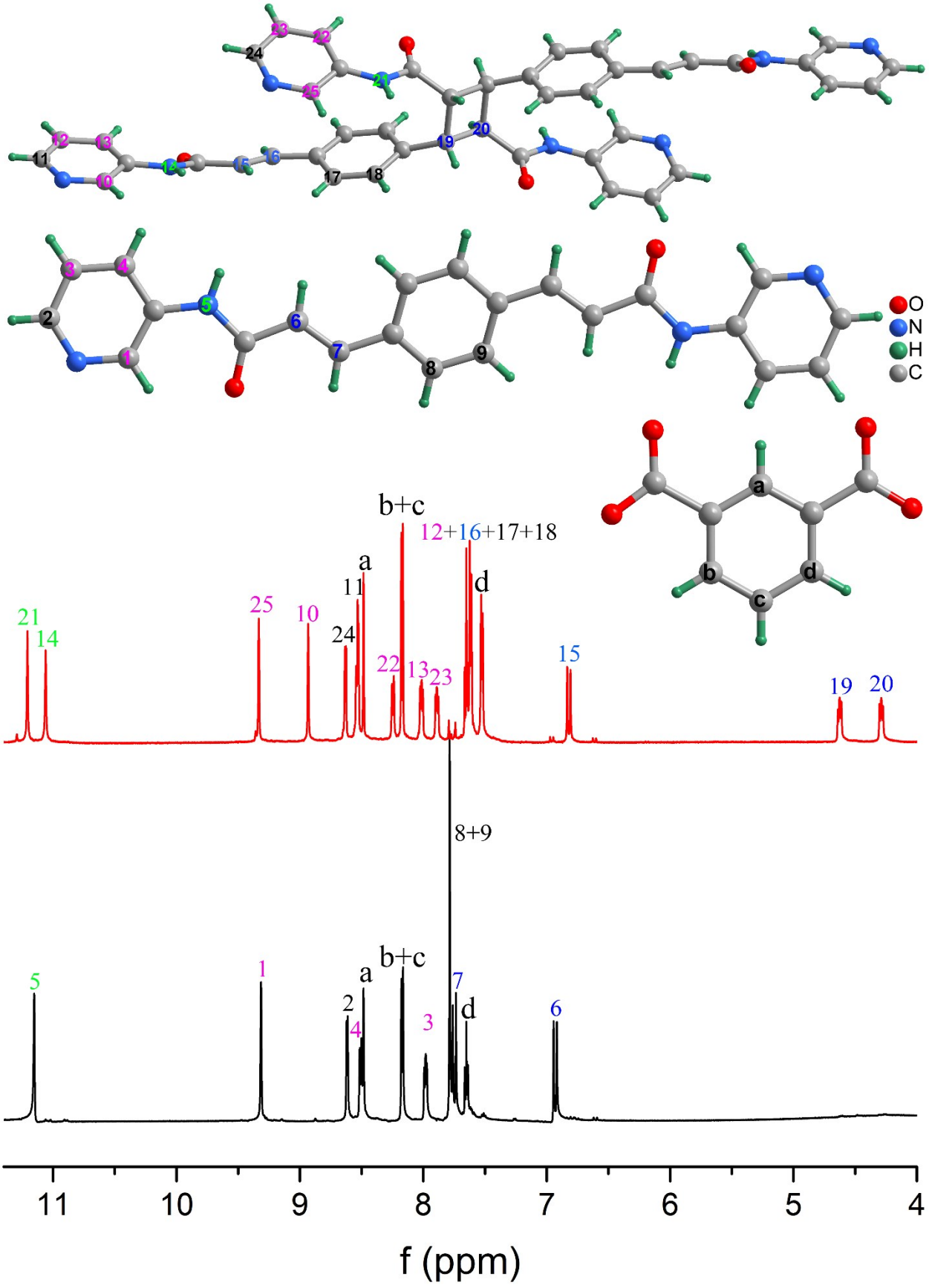


**Fig. S15** A comparison of the $^{1}$H-NMR spectrum of **1** and **1a** in DMSO-$d_6$.

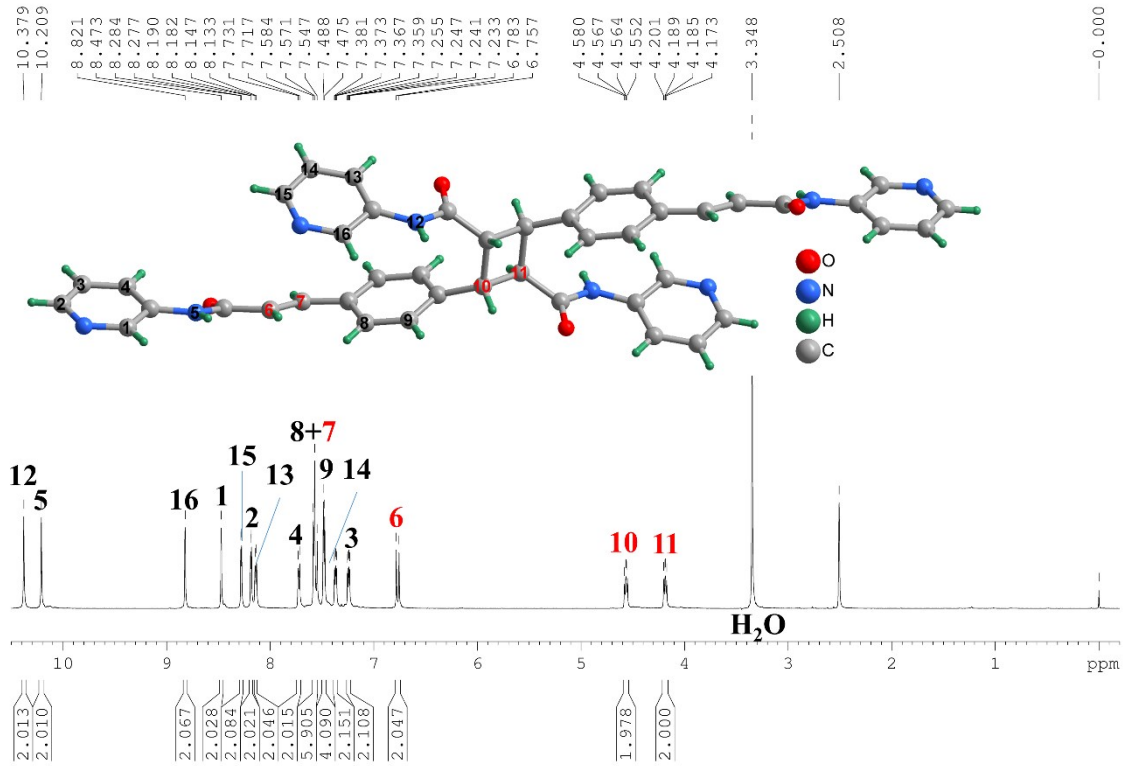


**Fig. S16** $^{1}$H-NMR spectrum of **babavpcb** in DMSO-$d_6$.

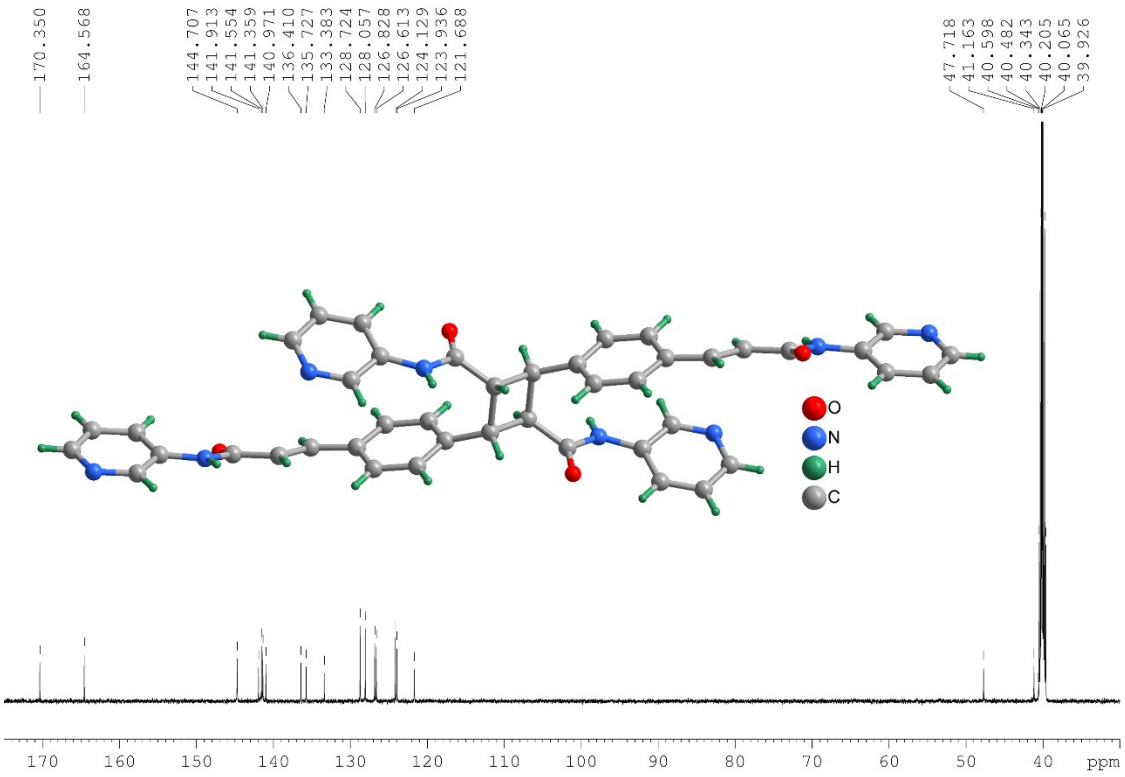


**Fig. S17** $^{13}$C-NMR spectrum of **babavpcb** in DMSO-$d_6$.

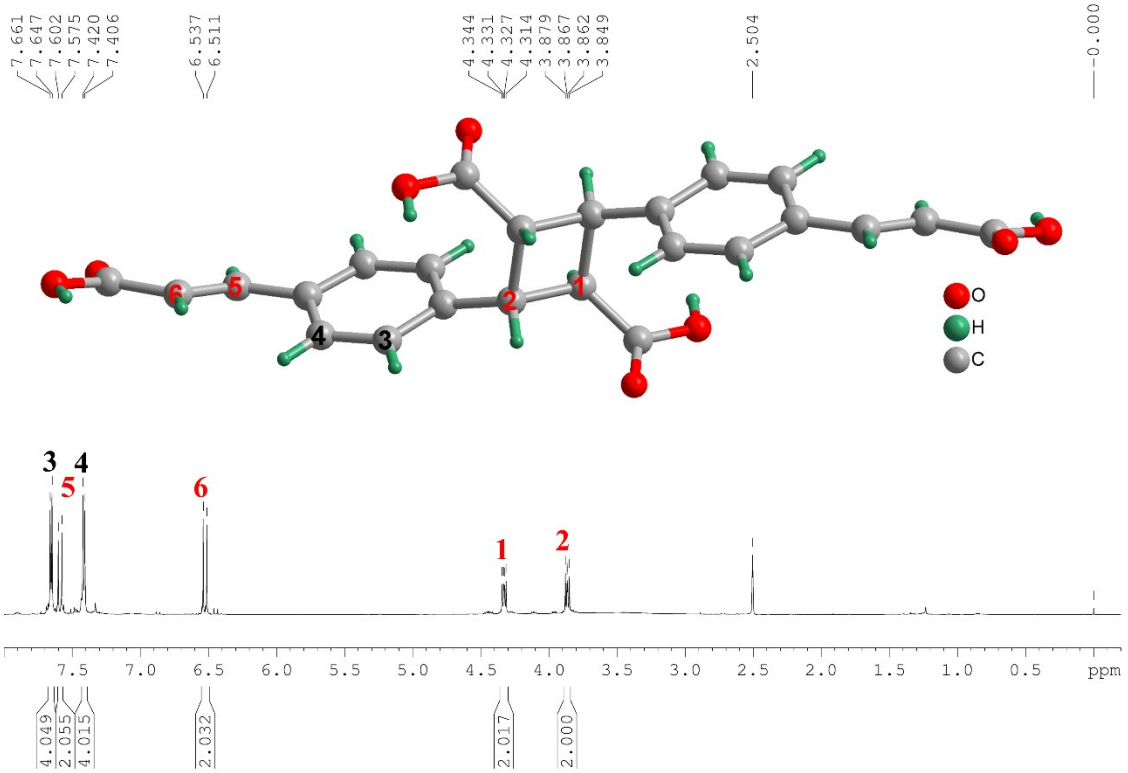


**Fig. S18** $^{1}$H-NMR spectrum of **bcbcvpcb** in DMSO-$d_6$.

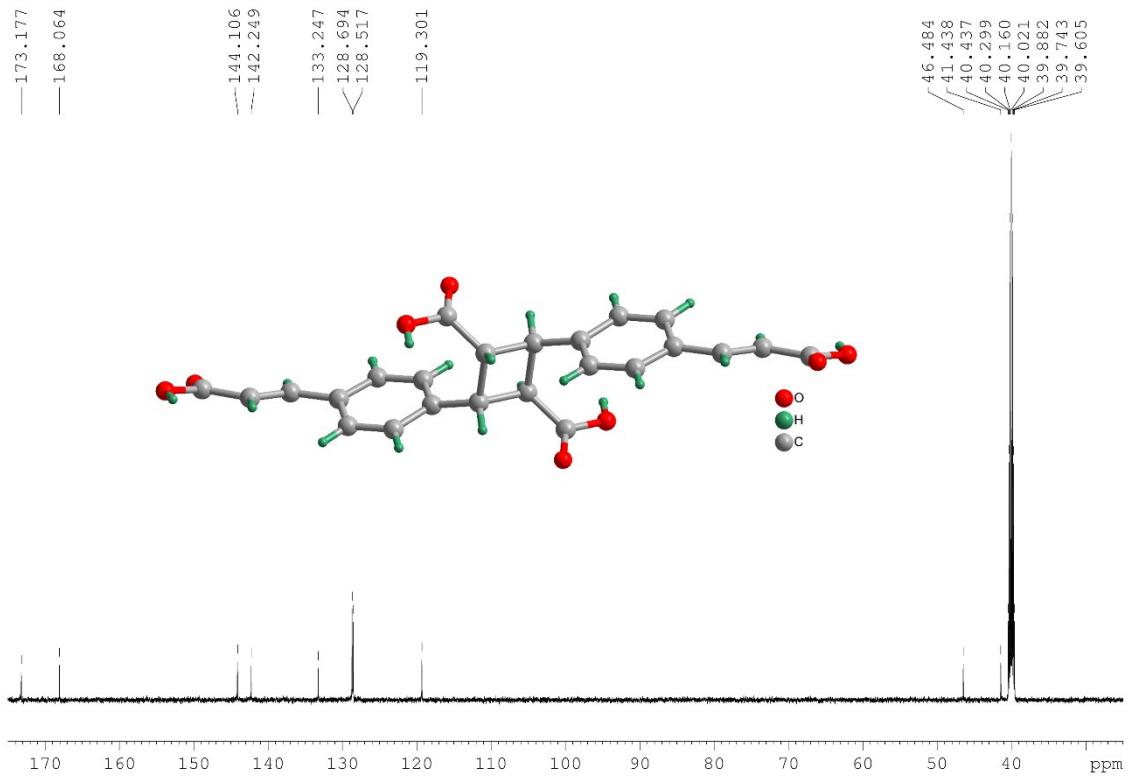


**Fig. S19** $^{13}$C-NMR spectrum of **bcbcvpcb** in DMSO-$d_6$.

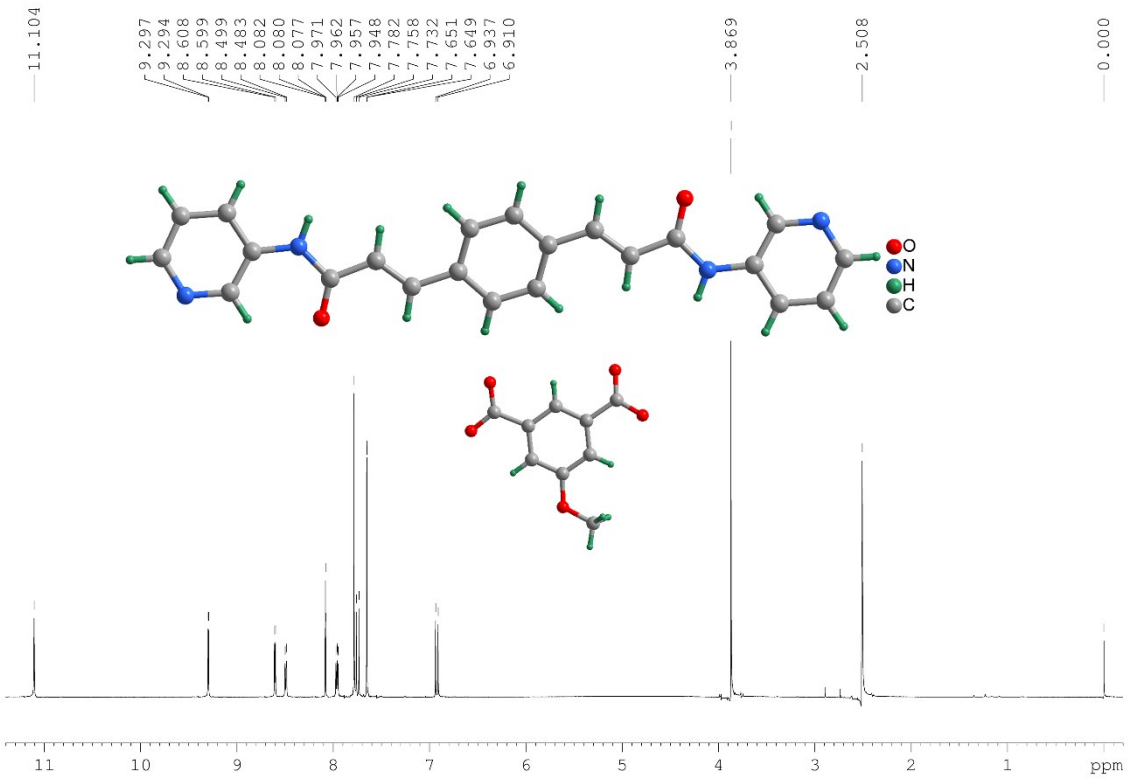


**Fig. S20** $^{1}$H-NMR spectrum of **2** in DMSO-$d_6$.

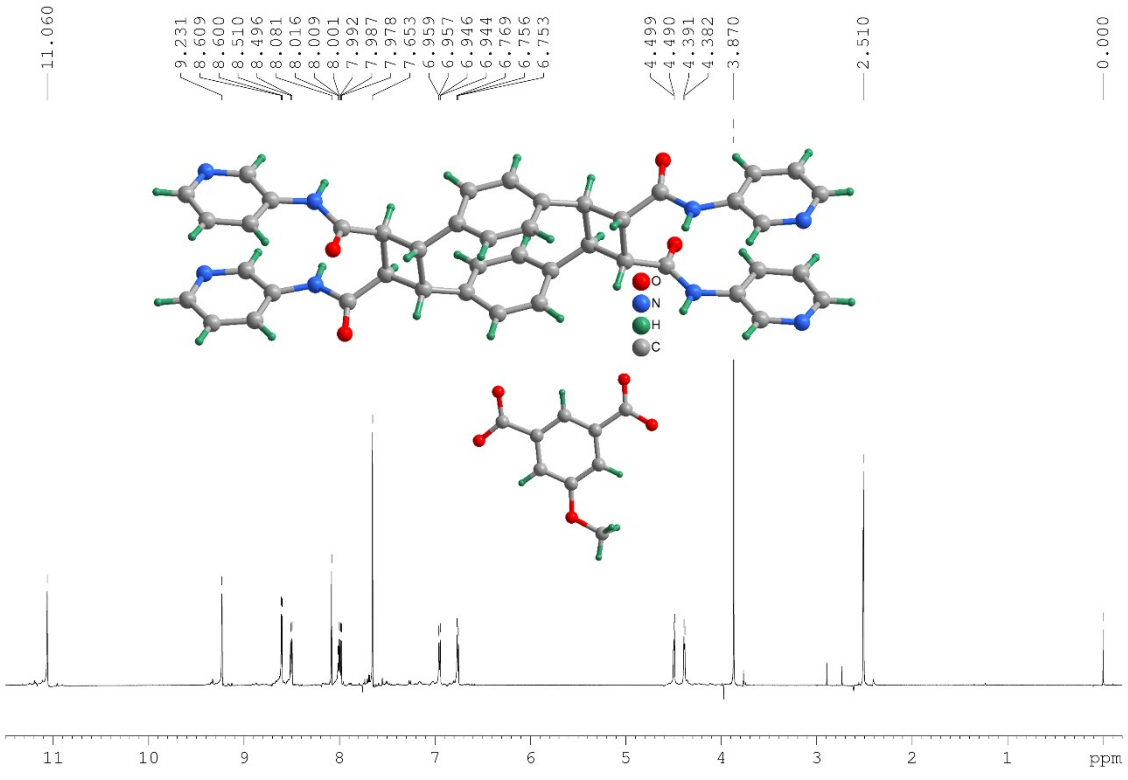


**Fig. S21** $^{1}$H-NMR spectrum of **2a** in DMSO-$d_6$.

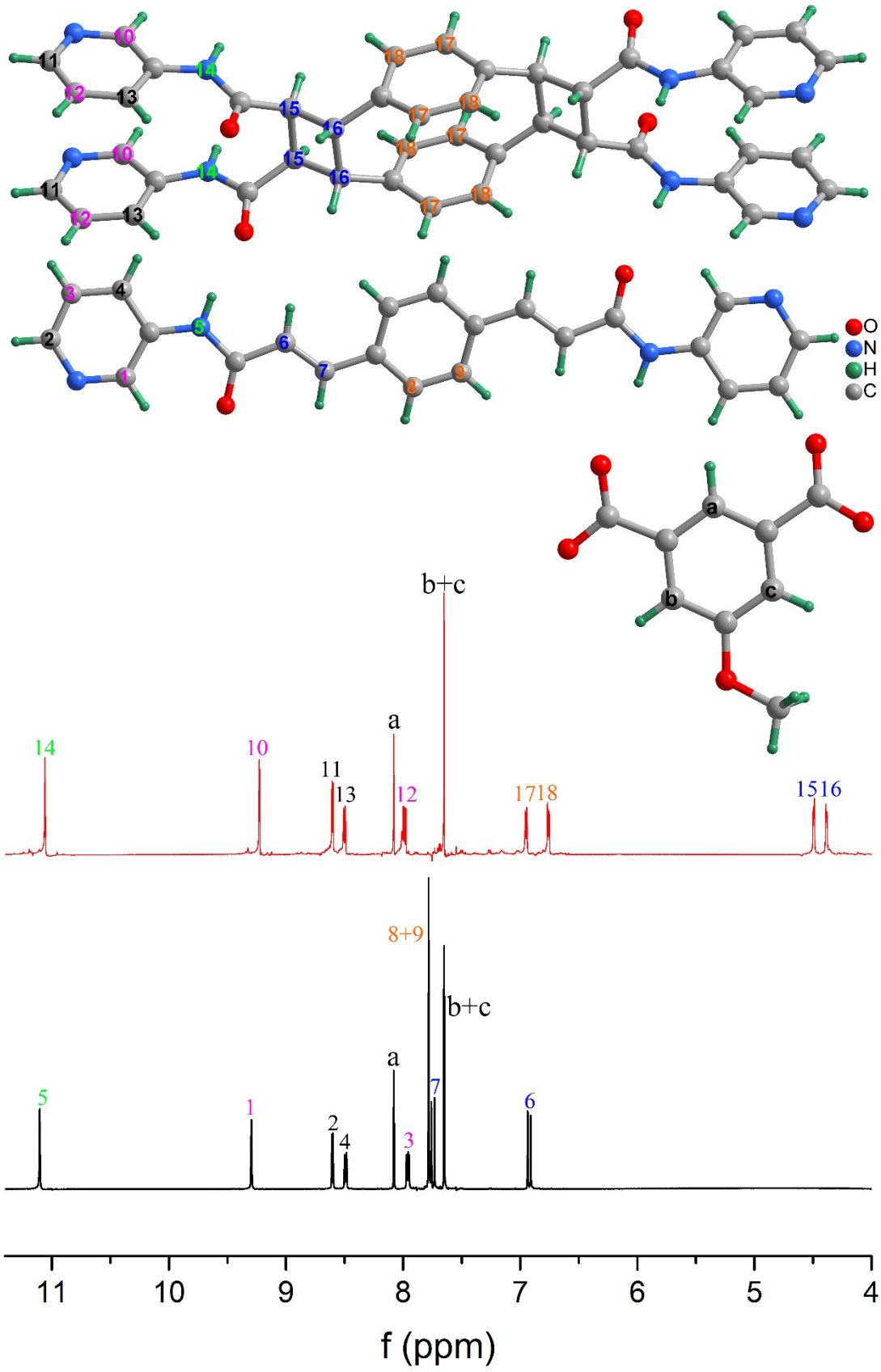


**Fig. S22** A comparison of the $^{1}$H-NMR spectra of **2** and **2a** in DMSO-$d_6$.

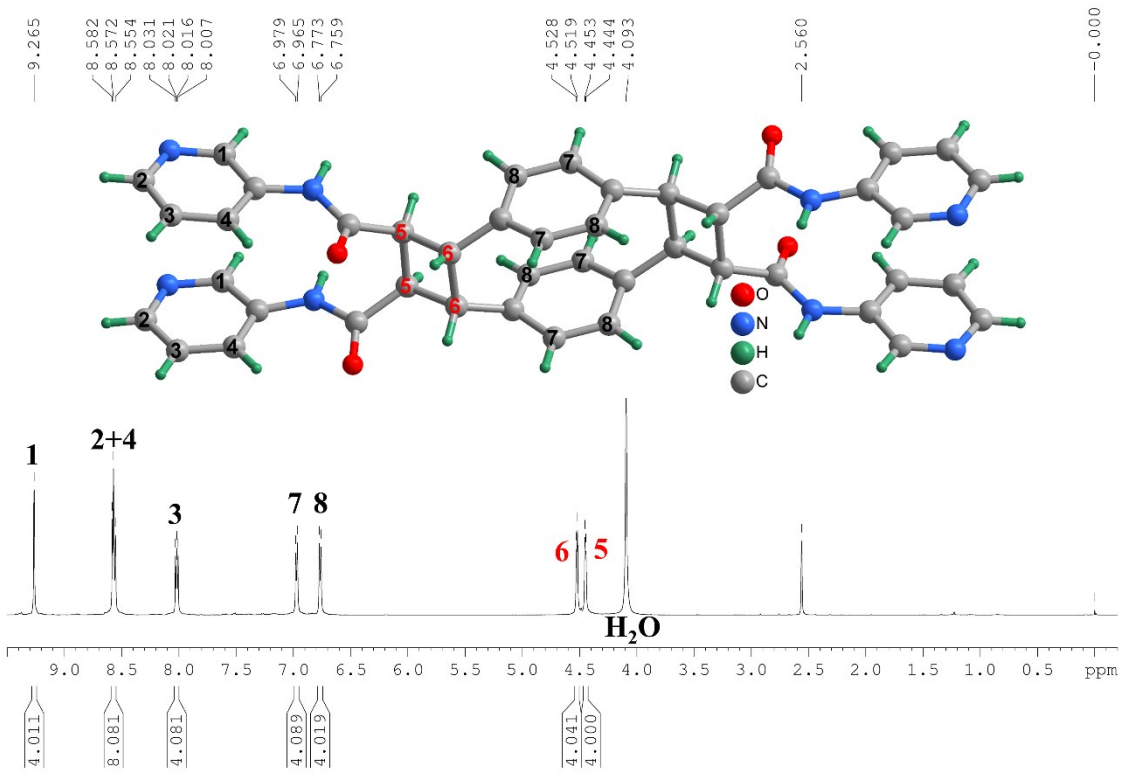


**Fig. S23** $^{1}$H-NMR spectrum of **tapcp** in DMSO-$d_6$ with 100 µL DCl to dissolve the sample.

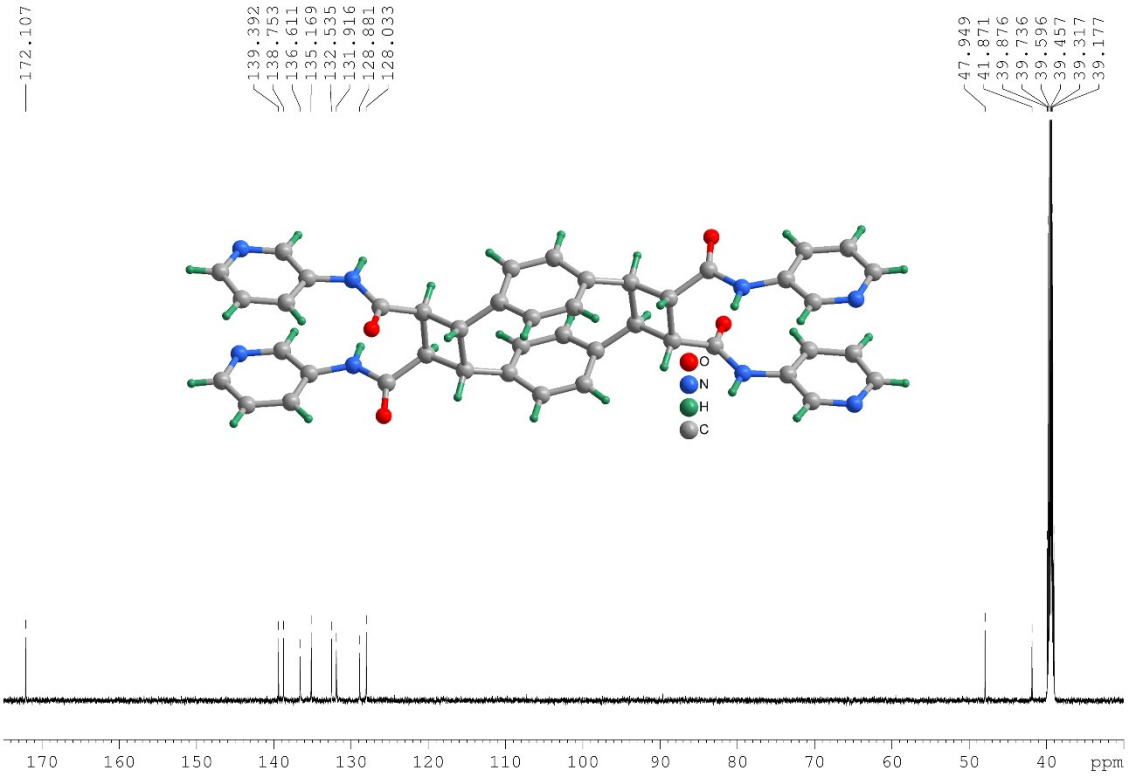


**Fig. S24** $^{13}$C-NMR spectrum of **tapcp** in DMSO-$d_6$.

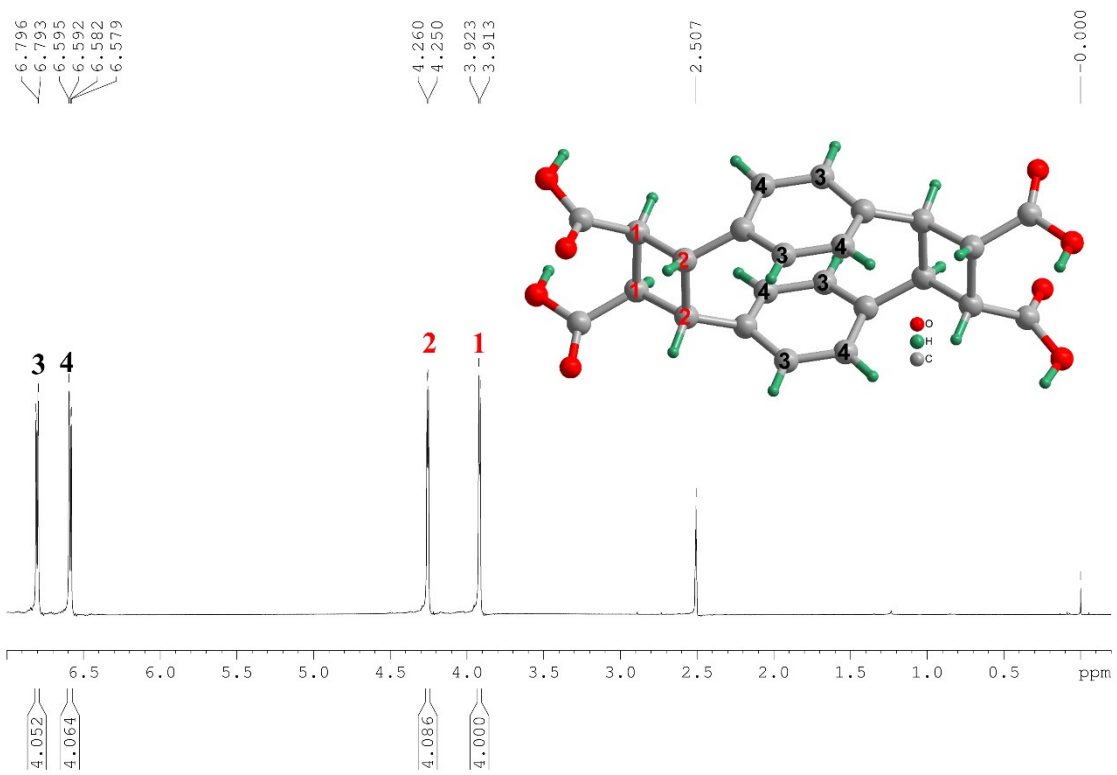


**Fig. S25** $^{1}$H-NMR spectrum of **tcpcp** in DMSO-d6.

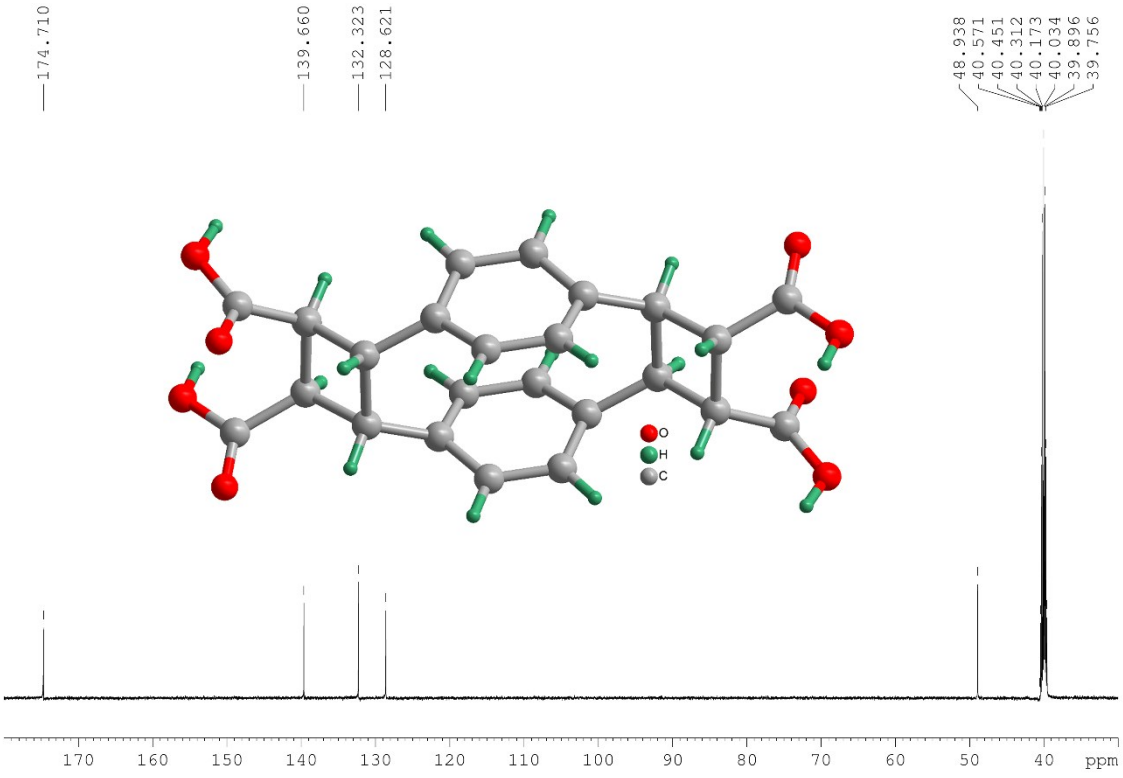


**Fig. S26** $^{13}$C-NMR spectrum of **tcpcp** in DMSO-$d_6$.

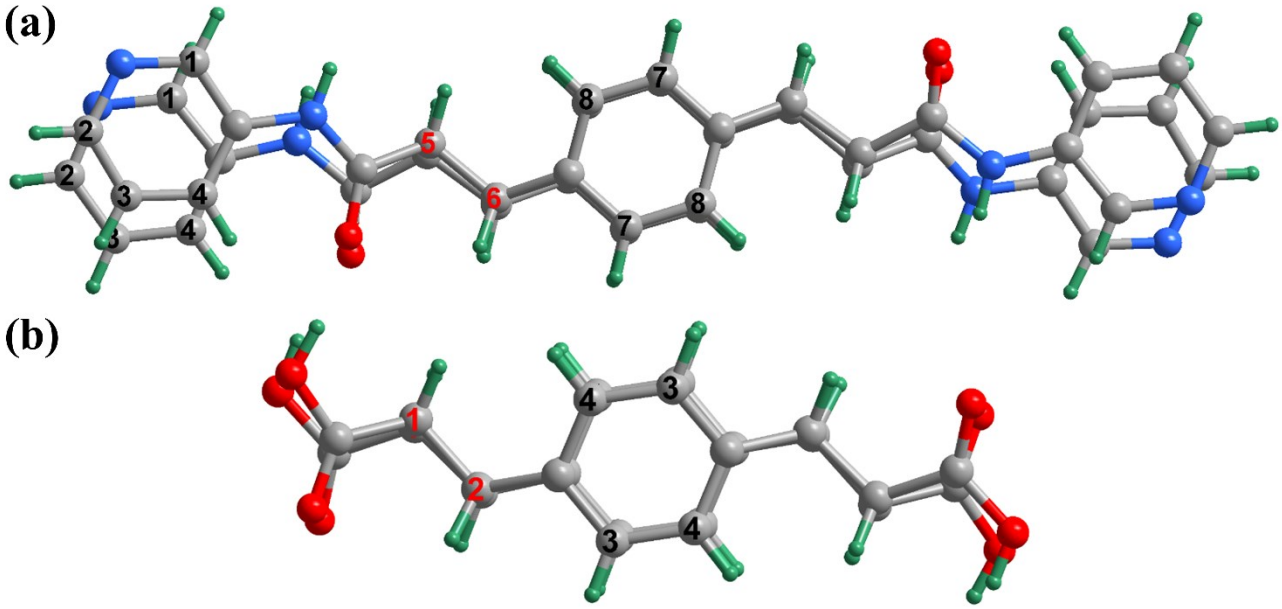


**Fig. S27** Molecular Structures of **tapcp** and **tcpcp**.

## Mass spectra

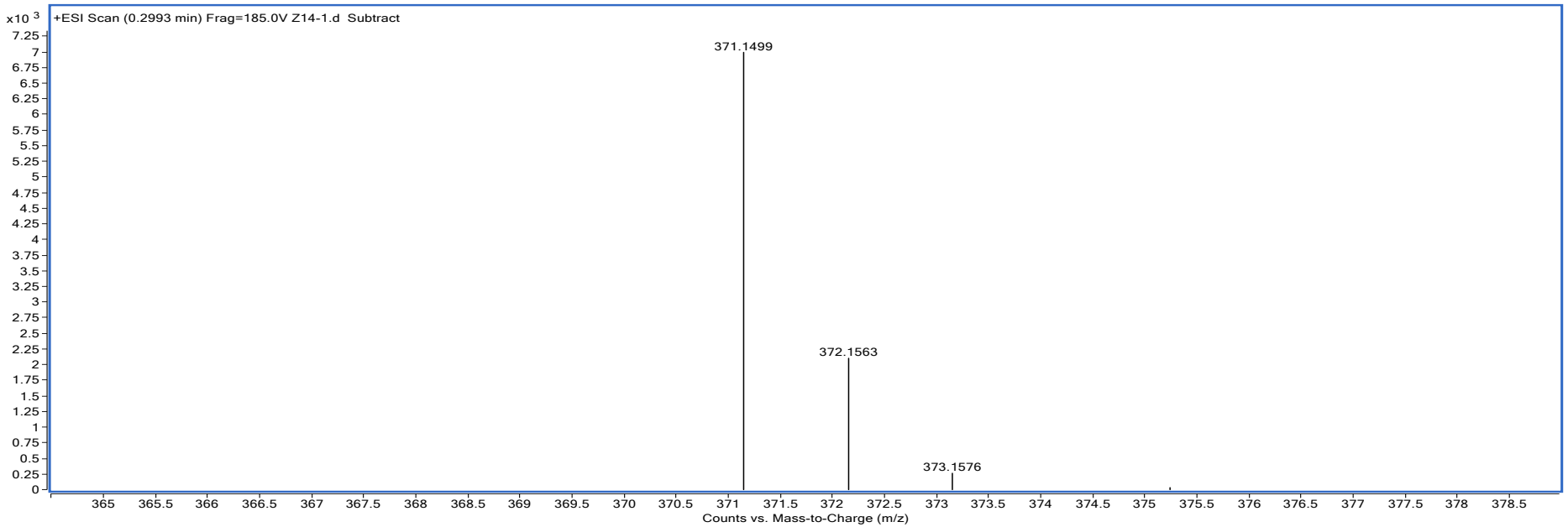


**Fig. S28** Positive–ion ESI mass spectrum of pbpa in DMSO.

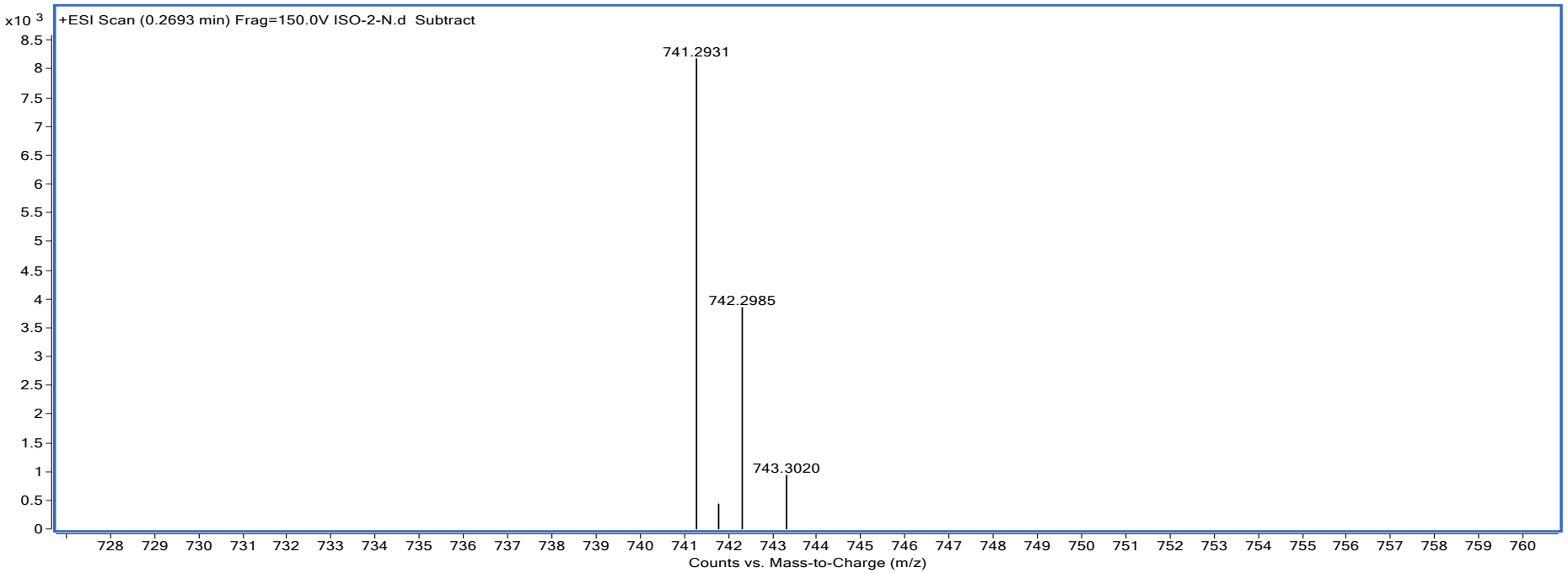


**Fig. S29** Positive–ion mass spectrum of babavpcb in DMSO.

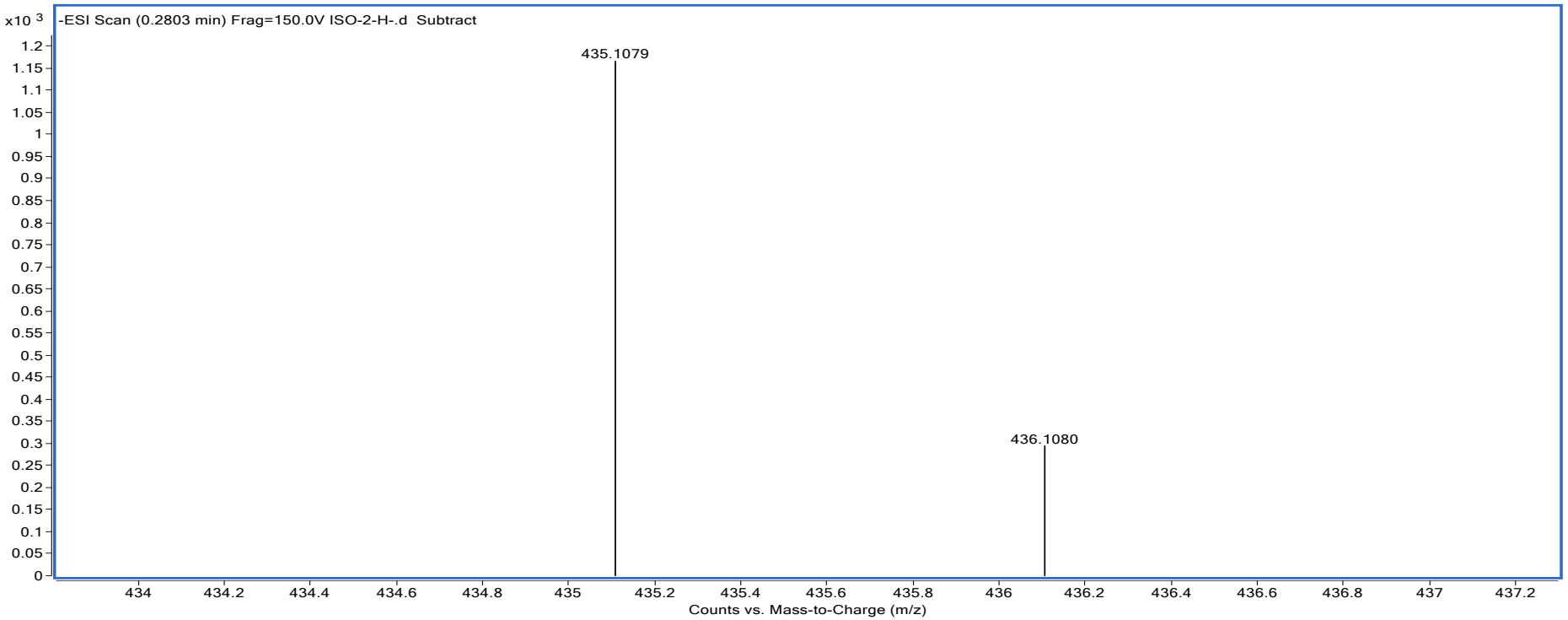


**Fig. S30** Negative–ion mass spectrum of bcbcvpcb in DMSO.

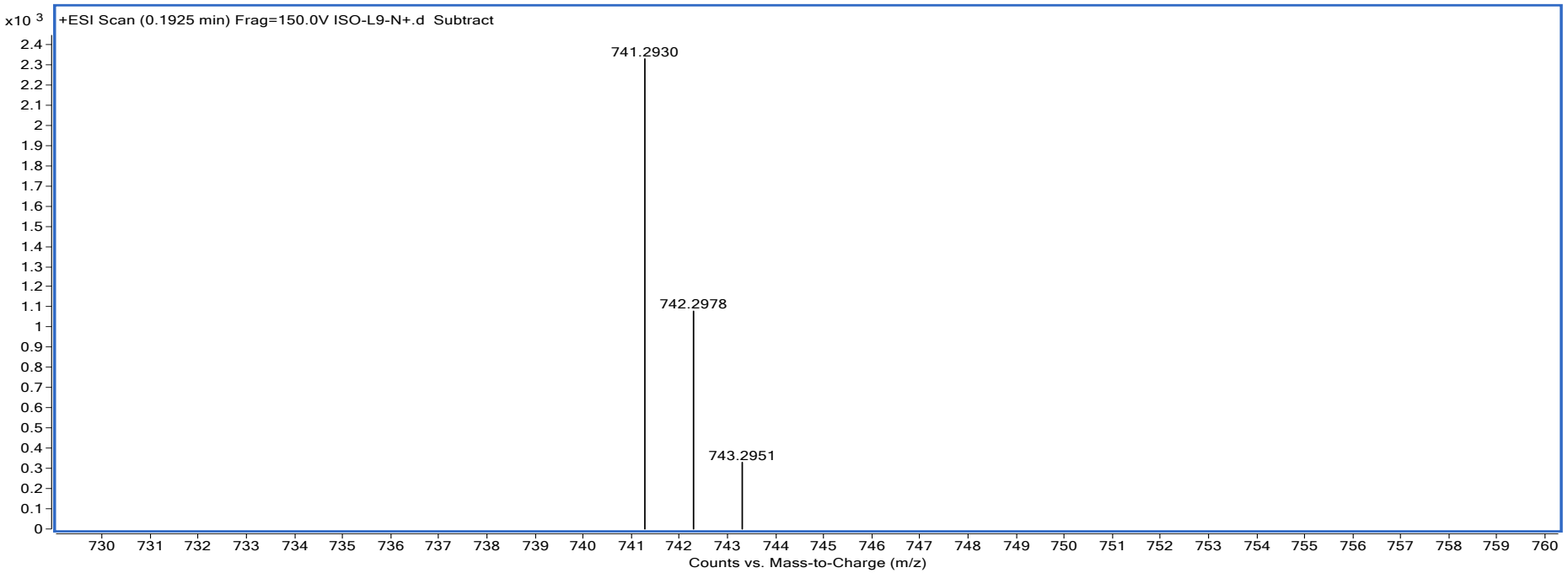


**Fig. S31** Positive–ion mass spectrum of tapcp in DMSO.

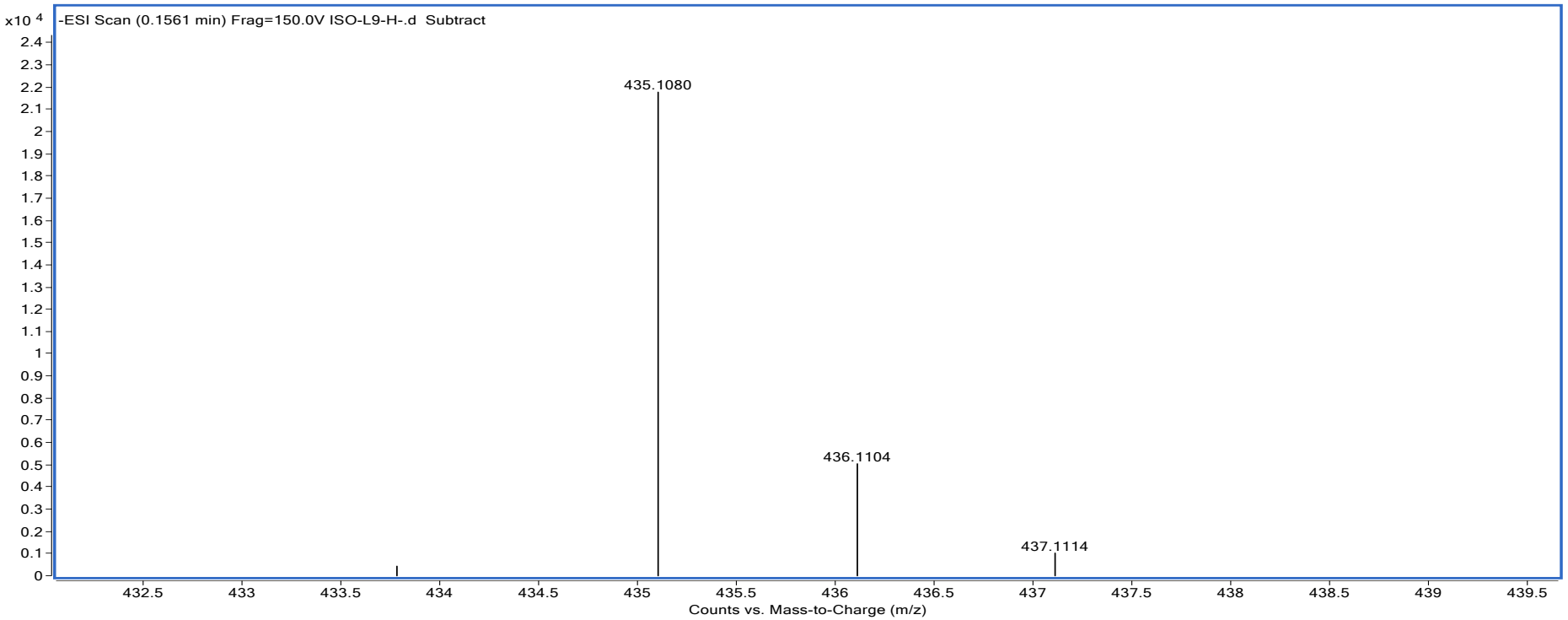


**Fig. S32** Negative–ion mass spectrum of tcpcp in DMSO.

**IR spectra**

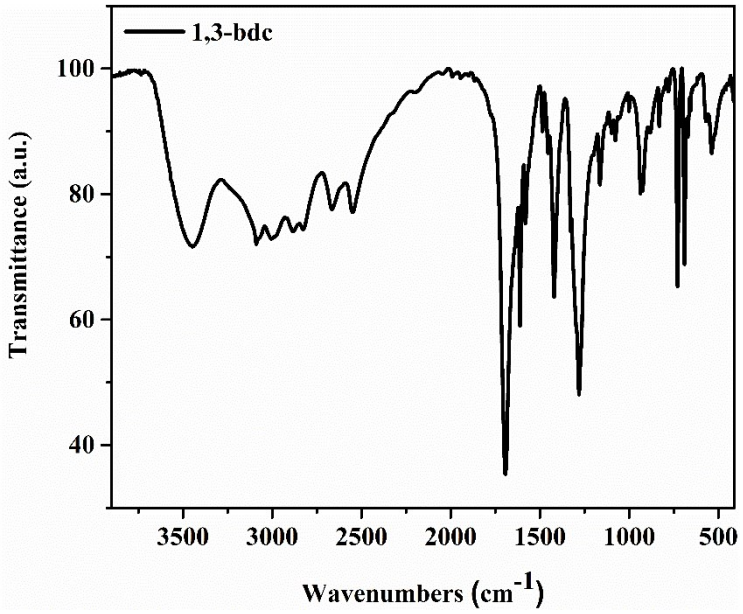


**Fig. S33** IR spectra of **1,3-bdc**.

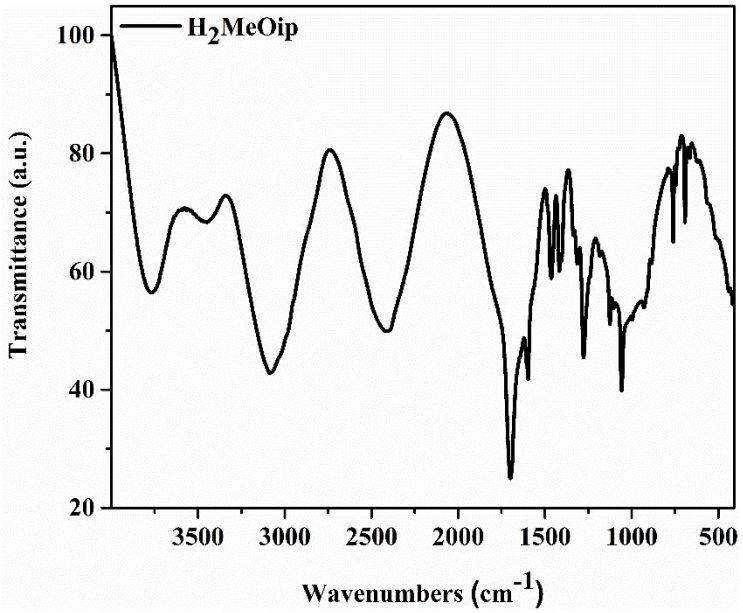


**Fig. S34** IR spectra of **$H_2$MeOip**.

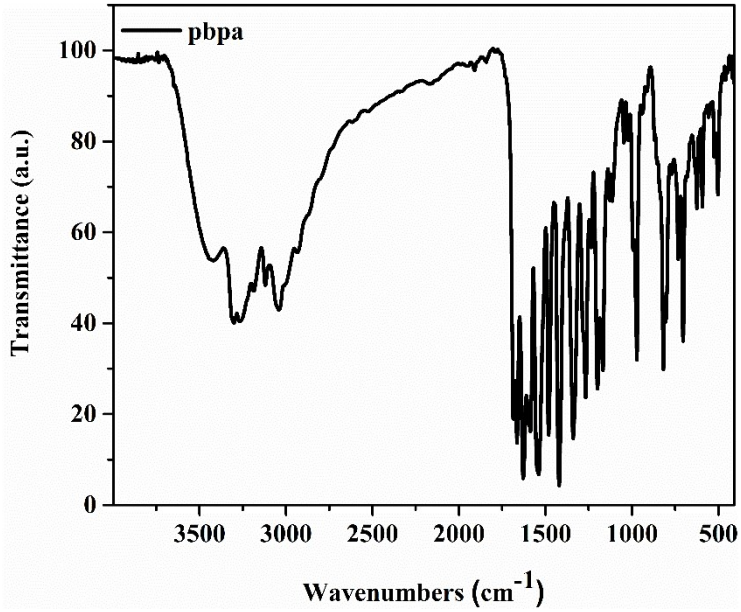


**Fig. S35** IR spectra of **pbpa**.

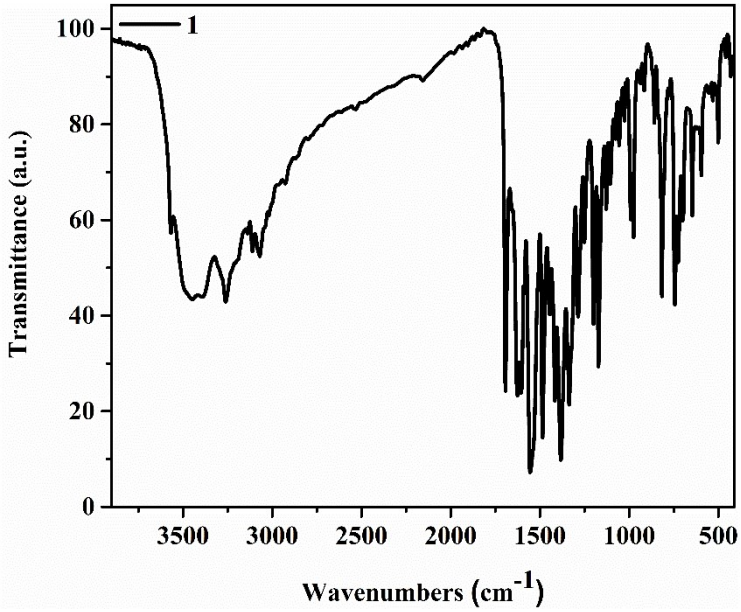


**Fig. S36** IR spectra of **1**.

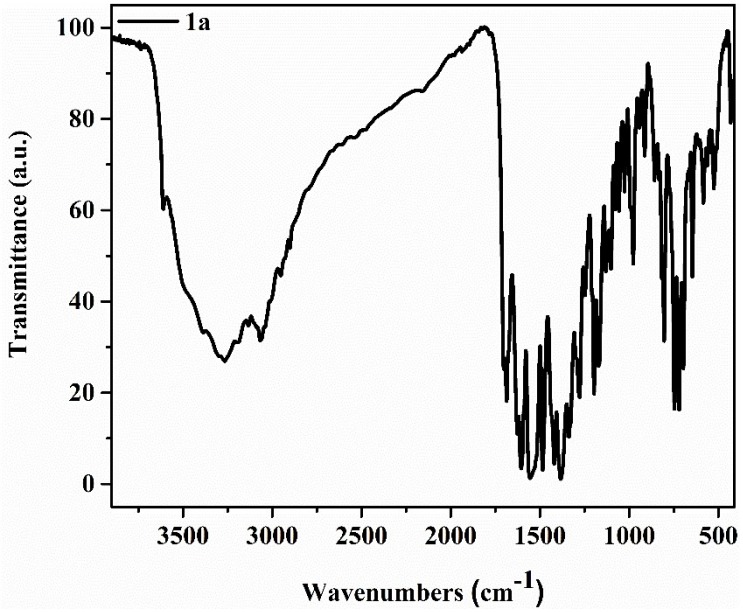


**Fig. S37** IR spectra of **1a**.

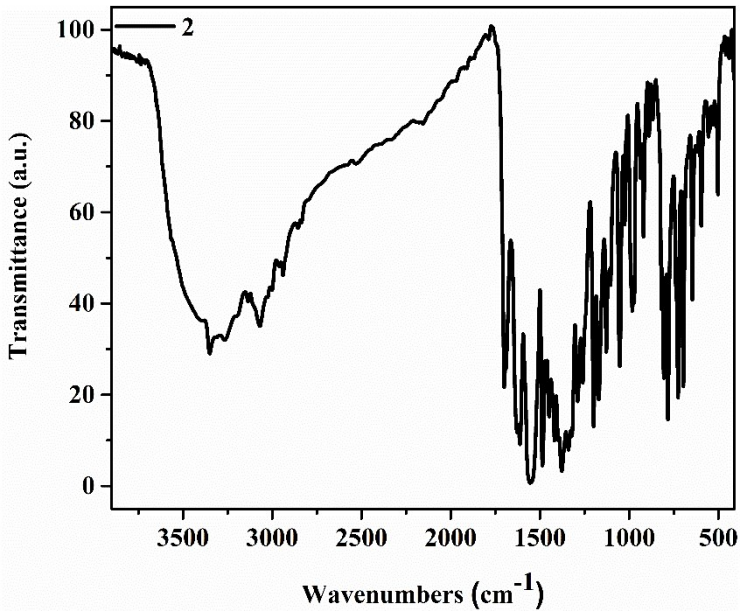


**Fig. S38** IR spectra of **2**.

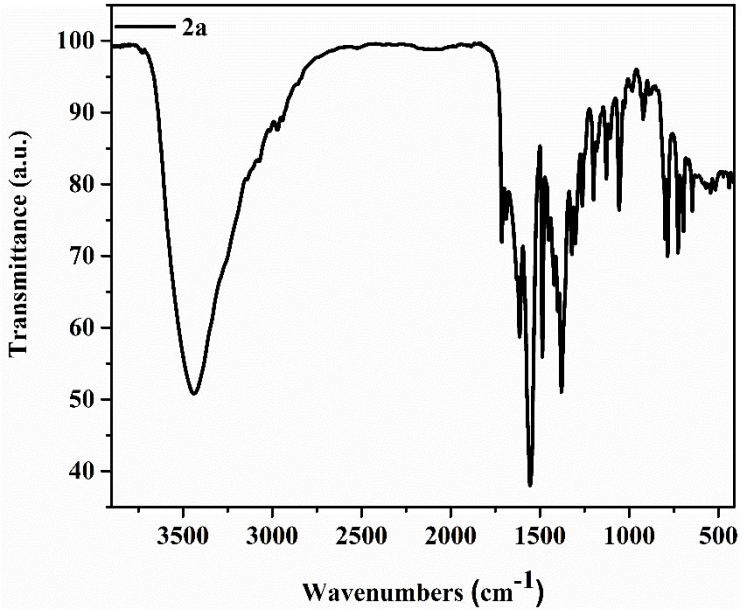


**Fig. S39** IR spectra of **2a**.

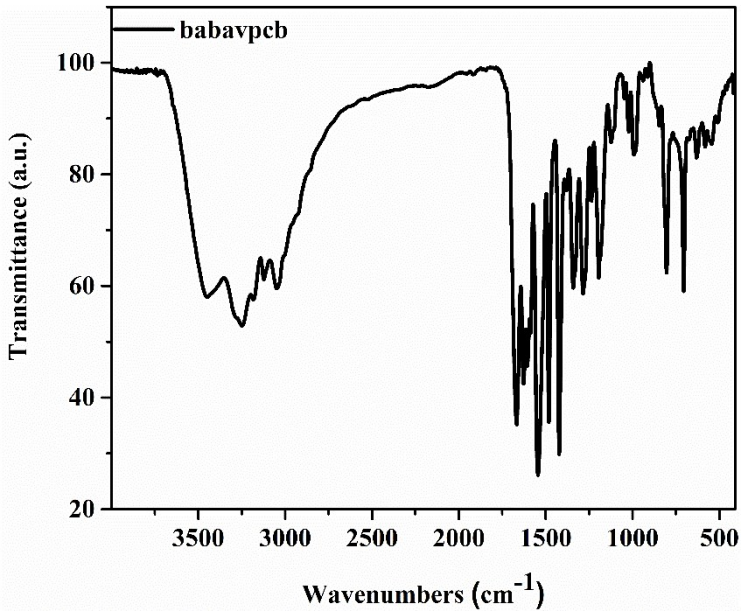


**Fig. S40** IR spectra of **babavpcb**.

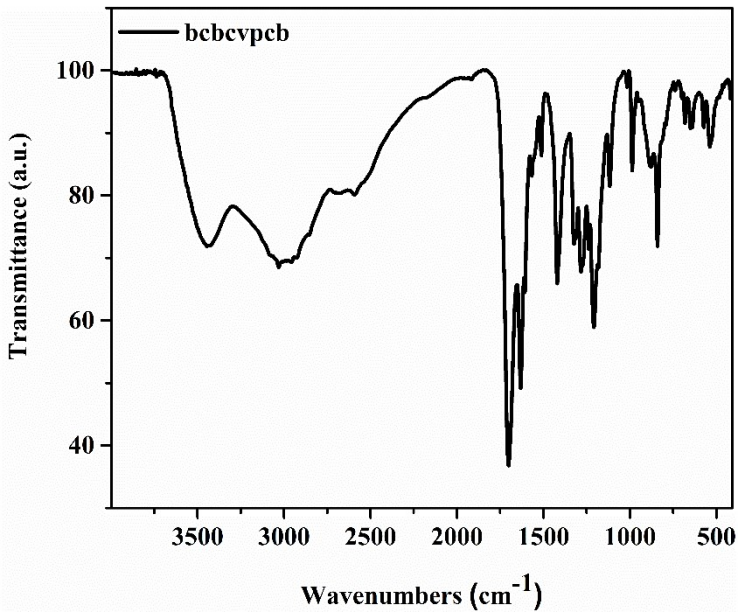


**Fig. S41** IR spectra of **bcbcvpcb**.

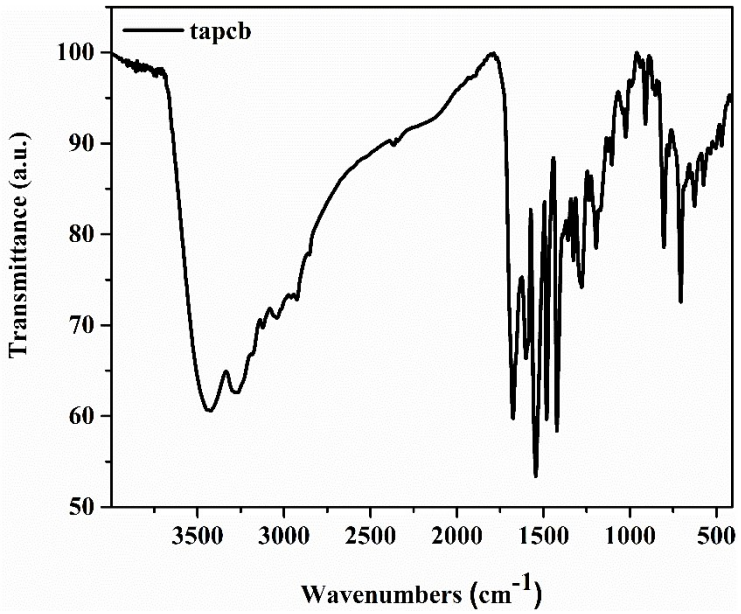


**Fig. S42** IR spectra of **tapcb**.

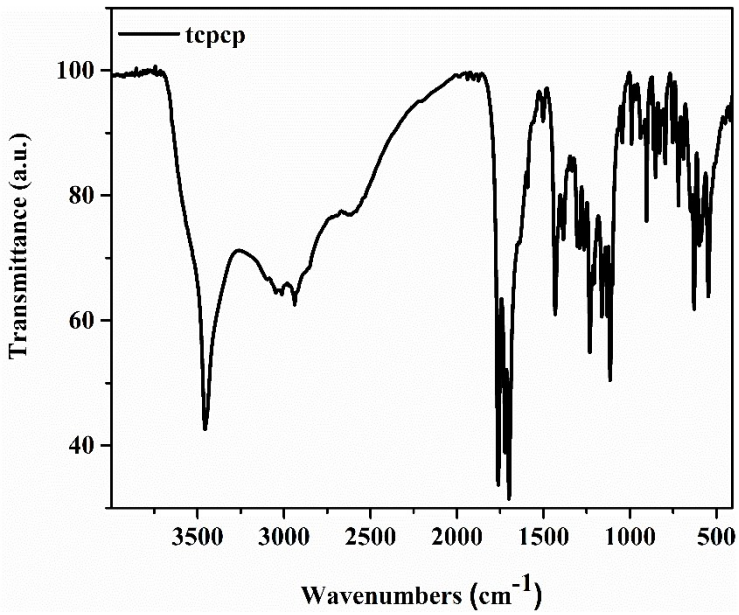


**Fig. S43** IR spectra of **tcpcb**.

## Thermo–gravimertic analysis (TGA)

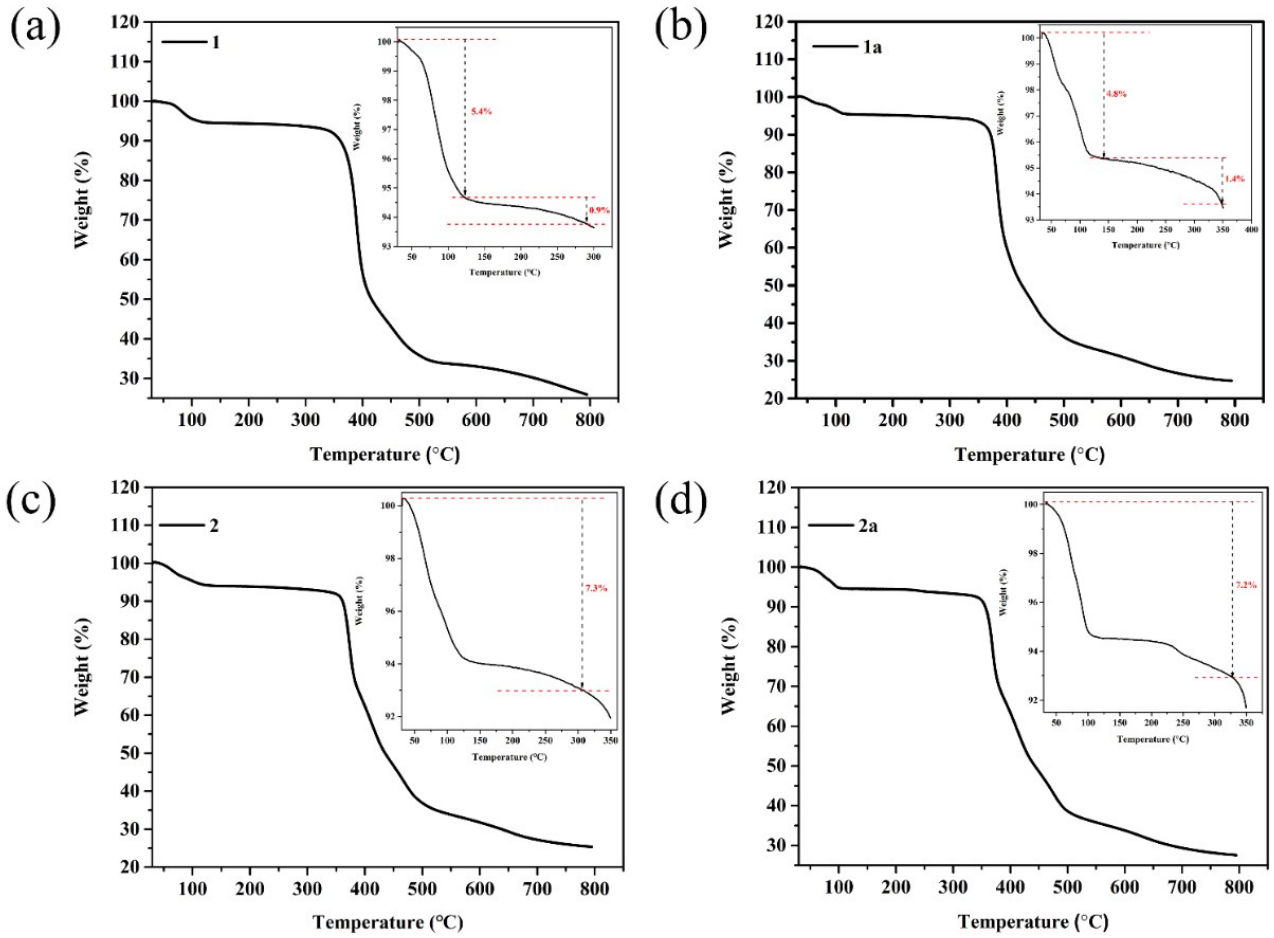


**Fig. S44** TGA of **1–2a**.

**Solid–state UV–visible absorbance spectra**

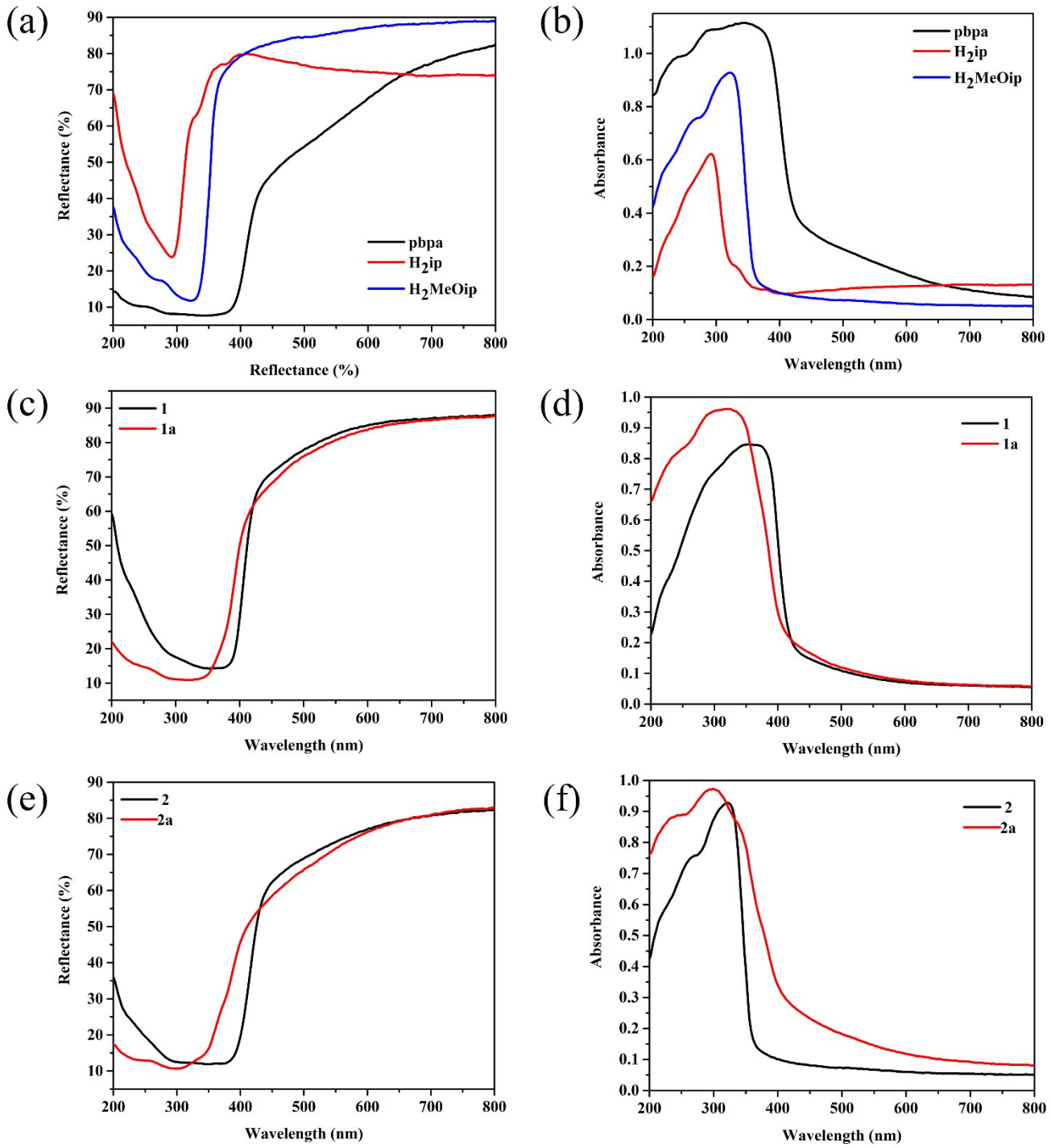


**Fig. S45** Solid–state UV–visible absorbance.

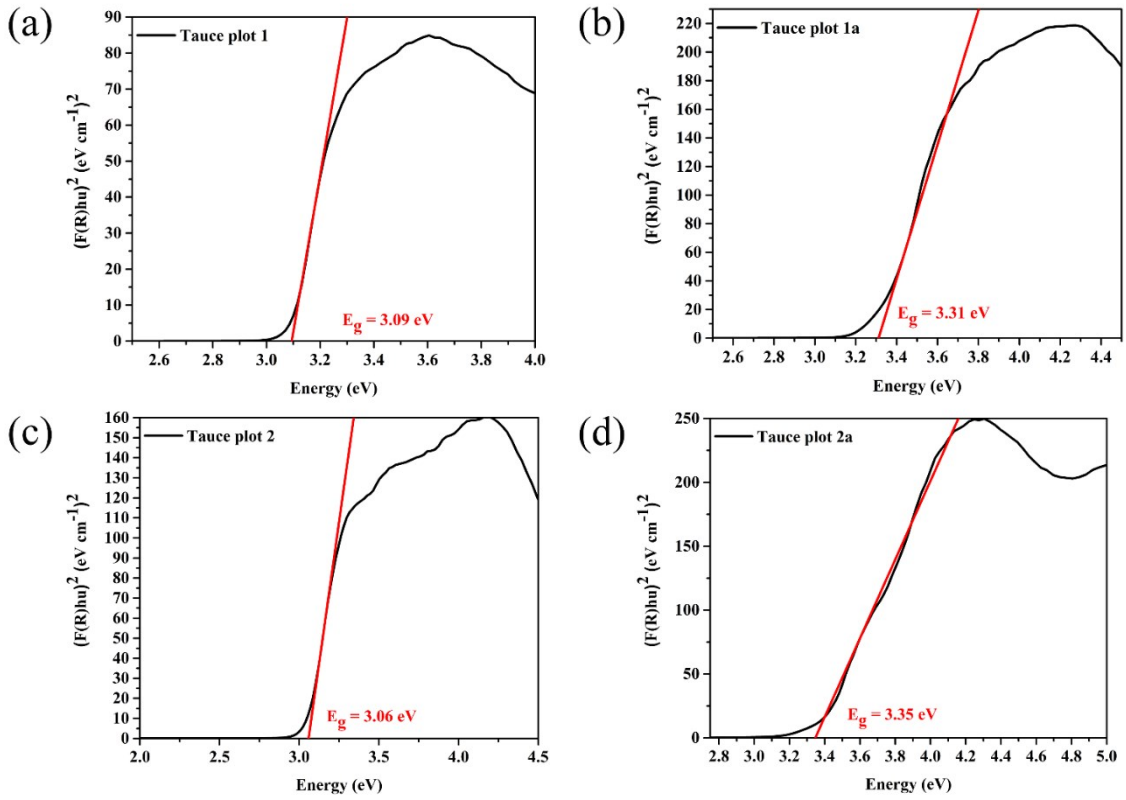


**Fig. S46** the direct optical band gap.

## Solid–state photoluminescence spectra

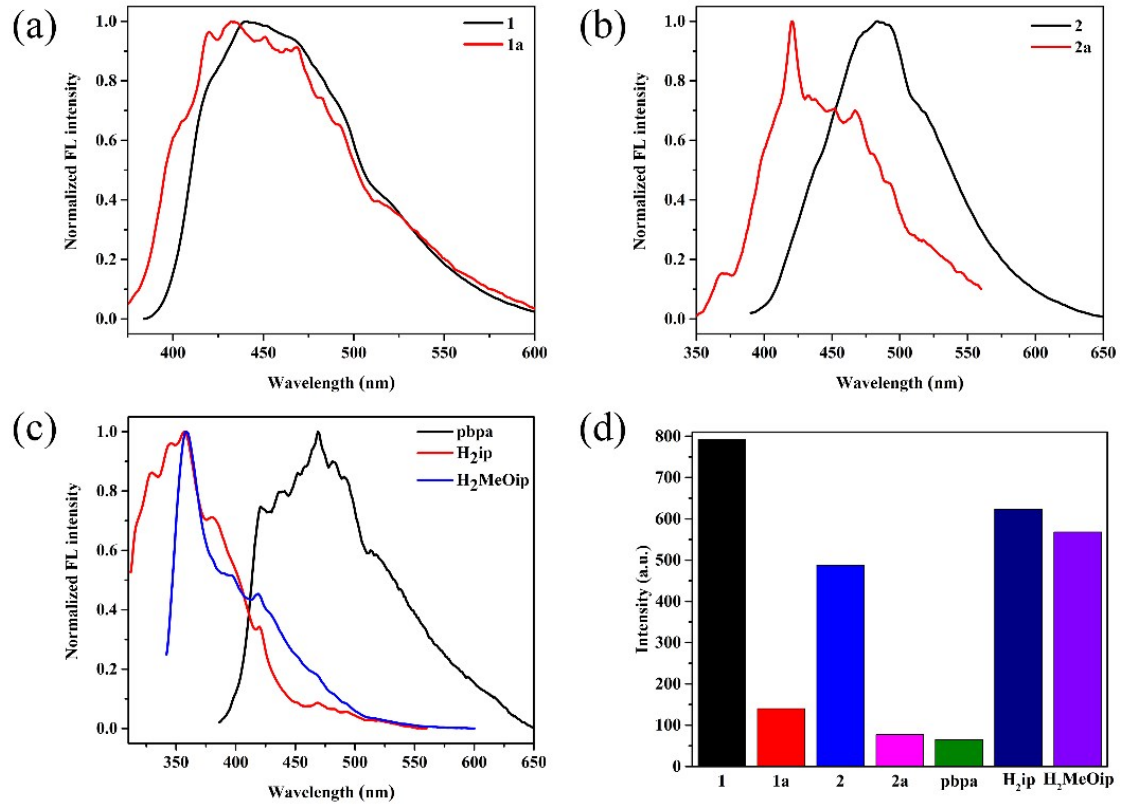


**Fig. S47** Normalized fluorescence spectra and fluorescence intensity.